PHYSICAL REVIEW D VOLUME 19, NUMBER 5 1 MARCH 1979

Production of jets and single particles at large transverse momentum in photon-photon collisions

S. J. Brodsky and T. DeGrand*
Stanford Linear Accelerator Center, Stanford University, Stanford, California 94305

J. Gunion
Department of Physics, University of California, Davis, California 95616

J. Weis
Department of Physics, University of Washington, Seattle, Washington 98195
(Received 19 October 1978)

Photon-photon collisions will be a copious source of jets and single particles produced with large transverse momentum in e^+e^- storage rings. These jets and single particles have topological properties which allow them to be easily distinguished from e^+e^- annihilation events. They arise from several sources: (a) quark exchange in $\gamma\gamma \to q\bar{q}$, (b) quantum-chromodynamics induced processes such as $\gamma_1 \to q\bar{q}$ and $\gamma_2 \to q\bar{q}$, with qq scattering via vector-gluon exchange, and (c) differential cross sections proportional to p_T^{-6} and p_T^{-8} at fixed $x_T = 2p_T/\sqrt{s}$ and fixed $\theta_{\text{c.m.}}$ characteristic of the constituent-interchange-model (CIM) picture. In particular, we predict $Ed\sigma/d^3p(e^+e^- \to e^+e^- + \text{jet} + X) \sim 0.03(1-x_T)p_T^{-4}$ nb GeV^2 for $p_T > 4$ GeV/c, characteristic of the simplest quark-exchange process, and $Ed\sigma/d^3p(e^+e^- \to e^+e^-\pi X) \sim (1-x_T)^2\, p_T^{-6}$ nb GeV^4 for $p_T > 2$ GeV/c, characteristic of the CIM subprocess $\gamma q \to \pi q$. Remarkably, the jet-trigger cross sections $Ed\sigma/d^3p(\gamma\gamma \to \text{jet} + X)$ turn out to be asymptotically scale-free and independent of $\alpha_s(p_T^2)$ when perturbative QCD contributions to all orders are included.

I. INTRODUCTION

It is well known that photon-photon inelastic collisions in e^+e^- storage rings become an increasingly important source of hadrons as the center-of-mass energy $\sqrt{s} = 2E_e$ is raised.[1] The dominant part of the cross section for $e^+e^- \to e^+e^-$ + hadrons arises from the annihilation of two nearly on-shell photons emitted at small angles to the beam. The resulting cross section increases logarithmically with energy ($m_e^2/s \to 0$, $s \gg m_H^2$) (Ref. 1):

$$d\sigma_{e^+e^- \to e^+e^- X}(s)/dm_H^2 \cong \frac{\alpha^2}{\pi^2} \ln^2\frac{s}{m_e^2}\,\frac{\sigma_{\gamma\gamma}(m_H^2)}{m_H^2}\ln\frac{s}{m_H^2}\,, \tag{1.1}$$

where m_H is the invariant mass of the produced hadronic system. In contrast, the e^+e^- annihilation cross section decreases quadratically with energy. For example, at the beam energy of $E_e = 15$ GeV, the standard vector-dominance estimate for $\sigma_{\gamma\gamma}(m_H^2)$ gives $\sigma(e^+e^- \to e^+e^- + \text{hadrons}) \cong 15$ nb for $m_H \geq 1$ GeV, compared to the annihilation cross section

$$\sigma_{e^+e^- \to \gamma \to \text{hadrons}} \equiv R\sigma_{e^+e^- \to \gamma \to \mu^+\mu^-} \cong (0.1\text{ nb})R\,.$$

If the hadronic interactions of a real photon are the same as those of a vector meson, then high-energy photon-photon collisions will be qualitatively similar to high-energy hadron-hadron collisions, with most hadrons produced with small momentum transverse to the beam direction. The study of such photon-photon reactions is of considerable interest since the entire range of hadronic phenomena can be studied for two incident spin-one bosons, whose mass and even linear polarization can be individually "tuned" when the e^+ and e^- are both tagged. Reviews of the various hadronic channels and theoretical predictions which can be probed in $\gamma\gamma$ collisions are given in Ref. 1.

Although vector-meson-dominance-model ideas are useful for low-momentum-transfer reactions, the production of hadrons at large transverse momentum is sensitive to processes where the photon's pointlike coupling to the quark current will dominate. In fact, because of the special role of the photon in quantum chromodynamics (QCD), we find that cross sections expected for jets of hadrons at large p_T are sizable, and are much larger than the extrapolation from hadron-hadron collisions.[2] For example, for $E_e = 15$ GeV, the total cross section for the production of jets with $p_T^J \geq 3$ GeV/c turns out to be of the order of 0.05 nb, i.e., the equivalent of $\frac{1}{2}$ unit of R.

This paper is devoted to a detailed study of high-p_T jet and single-particle production processes in $\gamma\gamma$ collisions, assuming the validity of QCD perturbation theory. In addition to being a pervasive background to e^+e^- annihilation studies at high-energy storage rings such as PEP and

PETRA, there are a number of important theoretical reasons why these reactions merit intensive study:

1. The elementary reaction $\gamma\gamma \to q\bar{q} \to$ hadrons yields a scale-invariant two-jet cross section at large p_T which is proportional to the fourth power of the quark charge. The corrections from higher-order QCD diagrams are of relative order $\alpha_c(4p_T^2)$. The observation of a two-jet scale-invariant cross section at the level predicted here will directly test the scaling of the quark propagator $\not{p}^{-1}$ at large p^2 in the $\gamma\gamma \to q\bar{q}$ subprocess.[3]

2. QCD processes which involve the large-p_T scattering of quark or gluon constituents are sensitive to the structure functions of nearly on-shell photons. Remarkably, as was first shown by Witten,[4] the photon structure function has a perturbative component which can be computed from first principles in QCD. At large q,[2,4,5]

$$G_{q/\gamma}(x, q^2) = \frac{\alpha}{\alpha_c(q^2)} f(x) + O(\alpha^2) . \tag{1.2}$$

Thus, aside from an overall logarithmic factor, the direct $\gamma \to q$ distribution displays exact Bjorken scaling. This result is accurate to all orders in $\alpha_c(q^2)$ (keeping only leading logarithms), and is in striking contrast to the pattern of scaling violations predicted in QCD for hadronic structure functions.

An important consequence of this result, first discussed by Llewellyn Smith,[5] is that processes such as $\gamma_1 \to q_1\bar{q}_1$, $\gamma_2 \to q_2\bar{q}_2$ with $q_1 + q_2 \to q_1 + q_2$ scattering at large p_T via gluon exchange leads to scale-invariant large-p_T jet cross sections; in fact, we shall show that the dependence on $\alpha_c(p_T^2)$ cancels out in the asymptotic cross section. This result is also true for the contribution of $\gamma q \to gq$ subprocesses.

3. The QCD analysis of large-momentum-transfer reactions for hadron-hadron collisions is subject to uncertainties due to possible nonperturbative effects, wee interactions, etc.[6] Such corrections are presumably absent when the direct pointlike couplings of the incident photons are involved.

4. In the case of single-particle production at large p_T, we predict that "higher-twist" subprocesses such as $\gamma_1 + q_2 \to$ meson $+ q$ dominate over fragmentation reactions such as $\gamma + \gamma \to q + \bar{q}$ with $q \to M + q'$ until very large p_T. The $\gamma q \to Mq$ subprocess is characteristic of the constituent-interchange model (CIM)[7] and breaks scale invariance by a power of p_T^{-2}.

5. The $\gamma\gamma$ process allows a study of the interplay between perturbative QCD processes and nonperturbative vector-dominance-model contributions, and (by utilizing tagged leptons at large angles) the transition between real-γ and virtual-γ reactions, including deep-inelastic scattering on a photon target. Furthermore, the onset of charm- and other heavy-quark thresholds can be studied once again from the perspective of $\gamma\gamma$-induced processes.

Thus the study of $\gamma\gamma$ collisions at large p_T provides a detailed laboratory for the study of QCD dynamics at short distances. We emphasize that the dominant hard-scattering processes in $\gamma\gamma$ collisions arise from the elementary-field nature of the photon and are particular to γ-induced reactions. The observation of such processes will provide unique and important tests of the basic subprocesses which govern large-transverse-momentum processes. While it has not been proved that the perturbative component and couplings of the real photon survive in the presence of confinement, we believe it is very likely. In vector-dominance language these contributions are represented by an infinite spectrum of massive vector mesons.[8] Here we shall approximate the hadronic interactions of the photon by combining the contributions of the lowest vector mesons (ρ, ω, ϕ) with the pointlike perturbative contribution. No serious double-counting error should occur since the pointlike interaction is equivalent to only very heavy vector mesons.

Jets induced by $\gamma\gamma$ reactions will show unmistakable signatures in colliding-beam experiments. Since the probability for γ emission by an electron into a given rapidity interval is essentially flat, the distribution of jets per rapidity interval will also be approximately flat and energy-independent away from the edge of phase space. Momentum conservation demands that a large-p_T jet on one side of a reaction must be balanced by one or more large-p_T jets on the away side. For the $\gamma\gamma \to q\bar{q}$ process one expects the production of two "SPEAR"-like jets each with total energy less than the c.m. energy $\sqrt{s}/2$. Because the rapidity of the $\gamma\gamma$ system is in general not zero, the jet events range from nearly back-to-back jets to a "V" configuration with a small opening angle along the beam axis. In all the other subprocesses the high-p_T jets are accompanied by additional jets of low-p_T hadrons from spectator particles which do not participate in the hard-scattering reaction.

Even without tagging the photon energies, the different contributing hard-scattering subprocesses can be distinguished by their topological jet structures, i.e., the number n_{jet} of hadronic jets observed in an event reflects the number of quark or gluonic systems initially separated. Specific examples are $n_{\text{jet}} = 2$ for $\gamma_1 + \gamma_2 \to q + \bar{q}$, $n_{\text{jet}} = 3$ for $\gamma_1 + q \to g + q$, $\gamma_1 + g \to q\bar{q}$ (where the incident quark

or gluon is a constituent of γ_2), $n_{\text{jet}}=4$ for $qq\to qq$, $gq\to gq$, etc. Gluon jets, quark jets, or hadronic resonances may be distinguishable by their leading particle structure and central region multiplicity density. In the case of $\gamma\gamma\to q\bar{q}$, the multiplicity should be nearly identical to that for $e^+e^-\to q\bar{q}$ at the same invariant $q\bar{q}$ energy.

In practice one will probably wish to reduce the background from the single-photon process by demanding that at least one lepton be observed at small angles in the final state. It will also be useful to have jet-tagging capability at small angles to differentiate between reactions which produce jets along the beam axis in addition to large-p_T jets.

It is instructive to compare photon-photon large-p_T processes with the corresponding reactions in hadron-hadron collisions. In the latter case, spectator particles are generally present so $n_{\text{jet}} \geq 4$. The dominant contribution to the jet cross section in hadron-hadron collisions is expected to arise from quark or gluon scattering via gluon exchange and to dominate nonscaling CIM (higher-twist) contributions for $p_T > 4$ GeV/c.[7,9] The cross section will be modified by logarithmic scale breaking from both $\alpha_c(4p_T^2)$ and the hadronic structure functions. In contrast, we find in photon-photon collisons that the jet cross section is dominated by the $n_{\text{jet}}=2$ subprocess for $p_T \geq 4$ GeV/c, and is asymptotically scale invariant. In hadron-hadron collisions, the single-pion cross section falls as p_T^{-8} at fixed $x_T = 2p_T/\sqrt{s}$ and fixed $\theta_{\text{c.m.}}$ for $2 \lesssim p_T \lesssim 8$ GeV/c, $20 \lesssim \sqrt{s} \lesssim 60$ GeV.[2] On the other hand, we expect single-meson cross sections for photon-photon collisions to behave as $p_T^{-6} f(x_T, \theta_{\text{c.m.}})$ for $1 \lesssim p_T \lesssim 10$ GeV/c, at PEP and PETRA energies. The observation of p_T^{-6} behavior in this domain for the $\gamma\gamma\to\pi X$ cross section is of particular interest since it would provide an important confirmation of the magnitude of the CIM contribution.

As the reader might imagine, a large number of different subprocesses are equally *a priori* important in generating large-p_T jets or mesons. We have had to develop a fairly general machinery for dealing with them, first introducing the parton model as a *modus operandi*, and then employing the hard-scattering expansion to group portions of Feynman graphs into hard-scattering subprocesses or into fragmentation functions. We then write down all possible hard scatterings and compute their (assumed to be incoherent) contributions to jet and single-particle cross sections. We can normalize all contributions since all coupling constants (α, α_c, and α_M, the $q\bar{q}M$ coupling in the CIM) are known or have been determined elsewhere at least to within a factor of 2 or 3.

We conclude the Introduction by summarizing the remainder of this paper. In Sec. II we introduce the theoretical framework which is necessary for describing jet or single-particle production at large p_T. Some details of the calculation are relegated to an appendix. In Sec. III we summarize the many subprocesses which contribute to large-p_T production, and quote both analytical expressions and approximate numerical estimations of their magnitude. In Sec. IV we combine all these results to present our predictions for jet and single-particle cross sections at $\sqrt{s}=30$ GeV, $\theta_{\text{c.m.}}=90°$. Finally, Sec. V contains our conclusions. Appendix B contains a detailed discussion on the QCD perturbative contribution to the photon structure function.

II. FORMALISM

A. Equivalent-photon approximation and the hard-scattering expansion

We will calculate the differential cross section for the scattering $e^+e^-\to e^+e^-\gamma\gamma\to e^+e^-$ (jet or π^+) X via the equivalent-photon approximation.[10] This technique is a useful method for obtaining the leading high-energy behavior of electroproduction cross sections where the scattered electron is either undetected or detected only if it is scattered into a small forward angle. The approximation consists of assuming that the emitted photon, which tends to emerge at small angle to the electron and with low invariant mass, is nearly massless, so that one can relate electroproduction cross sections to photoproduction cross sections. The cross section for the process $ee\to eeX$ in the equivalent-photon approximation is

$$d\sigma_{e^+e^-\to e^+e^-X}(s,t,u)=\int_0^1 dx_1\int_0^1 dx_2 N(x_1)N(x_2)\, d\sigma_{\gamma\gamma\to X}(\hat{s}=x_1x_2s,\ \hat{t}=x_1t,\ \hat{u}=x_2u)\,, \tag{2.1}$$

where $N(x)$ is the equivalent-photon energy spectrum and $d\sigma_{\gamma\gamma\to X}$ is the differential cross section for the scattering of two oppositely directed unpolarized photons (of energy $x_1\sqrt{s}/2$, $x_2\sqrt{s}/2$ in

the e^+e^- c.m. system) into a final state X. When x_1 and x_2 are computed as light-cone momentum fractions (see below), then Eq. (2.1) is invariant for Lorentz transformations along the beam direction.

The validity of the equivalent-photon approximation as compared to exact calculations has recently been examined by Ref. 11. When the full form of the equivalent-photon energy spectrum $N(x)$ is used the double equivalent-photon approximation was found to be a very good approximation for the process $e^+e^-\to e^+e^-\mu^+\mu^-$. For our purposes here we use the approximate form

$$N(x)\approx\left(\frac{\alpha}{2\pi}\ln\frac{s}{4m_e^2}\right)\frac{1+(1-x)^2}{x}\ , \tag{2.2}$$

where only the dominant logarithm is retained. The equivalent-photon approximation (2.2) is exact in the limit $m_e^2/s\to 0$ to lowest order in α.

The next ingredient which we will use in our calculations is the hard-scattering expansion, which is a technique for evaluating Feynman diagrams in large-momentum-transfer processes.[12] In a given Feynman graph, when a large-p_T particle is produced, there are generally many paths along which large momentum can flow. The hard-scattering expansion consists of isolating the portion of the graph in which the major part of the hard scattering occurs and labeling it as a scattering subprocess, while lumping the rest of the diagram, where only small momentum transfers occur, into fragmentation functions. This process is carried out while isolating all possible regions where the hard scattering may occur resulting in a sum of terms. For model field theories, the application of this procedure has been shown to reproduce the results of specific Feynman-graph calculations to within about 90% accuracy.[12]

Consider a contribution to the hard-scattering expansion where the constituents a and b of the initial particles A and B, respectively, undergo a hard scattering to produce a particle or jet C at large transverse momentum. A simple parton formula holds for each such contribution:

$$\frac{Ed\sigma}{d^3p}(AB\to CX)=\int_0^1\int_0^1 dx_1dx_2G_{a/A}(x_1)G_{b/B}(x_2)\times\frac{d\sigma}{dt}(ab\to Cd)\frac{\hat{s}}{\pi}\delta(\hat{s}+\hat{t}+\hat{u})\ , \tag{2.3}$$

where the fragmentation function $G_{i/I}(x_i)$ gives the probability of finding a parton i of light-cone momentum fraction $x_i\equiv(p_i^0+p_i^3)/(P_I^0+P_I^3)$ in the particle I. The invariants are

$$s\equiv(p_A+p_B)^2,\quad t=(p_A-p_C)^2,\quad u=(p_B-p_C)^2\ , \tag{2.4}$$

and

$$\begin{aligned}\hat{s}&\equiv(p_a+p_b)^2\approx x_1x_2s\ ,\\ \hat{t}&\equiv(p_a-p_c)^2\approx x_1t\ ,\\ \hat{u}&\equiv(p_b-p_c)^2\approx x_2u\ .\end{aligned} \tag{2.5}$$

Here the particles A and B are the initial e^+ and e^-. In the case that a and b are photons, Eq. (2.3) is identical to Eq. (2.1) where $G_{\gamma/e}(x)=N(x)$. However, generally the partons a and b participating in the hard scattering may be constituents of the photons rather than the photons themselves. In this case $G_{a/e}$ is obtained from the convolution of $G_{\gamma/e}$ with the probability of finding the given constituent in the photon. Many different fragmentation functions and subprocess differential cross sections may in principle be important. Our task will be to elucidate precisely which of them are, in fact, most important.

B. Fragmentation functions

We now discuss the fragmentation functions which we will use in the convolution integral, Eq. (2.3). This is most easily done by discussing the simplest fragmentation functions separately and building the more complicated ones from them by the convolution formula

$$G_{a/c}(x)=\int_x^1\frac{dz}{z}G_{b/c}(z)G_{a/b}\left(\frac{x}{z}\right)\ . \tag{2.6}$$

For ease in evaluating the convolution integral it is convenient to normalize a fragmentation function as

$$xG_{a/b}(x)=\sum_i\Lambda_i(1+g_a^{(i)})(1-x)^{g_a^{(i)}} \tag{2.7}$$

and quote values for Λ.

The simplest fragmentation functions are those for photon emission by electrons and for photon annihilation into an electron-positron pair. In the leading-logarithmic approximation to the equivalent-photon approximation, the probability for an electron to emit a (transversely polarized) photon with transverse momentum $\vec{k}_T$ and longitudinal-momentum fraction x is

$$\frac{dN}{dxd^2k_T}\equiv G_{\gamma/e}(x,\vec{k}_T)=\frac{\alpha}{2\pi^2}\frac{k_T^2}{(k_T^2+x^2m_e^2)^2}\frac{1+(1-x)^2}{x} \tag{2.8}$$

or integrating on $\vec{k}_T$,

$$G_{\gamma/e}(x)=\frac{\alpha}{2\pi}\ln\eta\left(\frac{1+(1-x)^2}{x}\right), \tag{2.9}$$

where $\eta=s/4m_e^2$ if the electron is not tagged, and $\theta_{\max}^2/\theta_{\min}^2$ if the electron is constrained to lie in an angle θ between $\theta_{\max}$ and $\theta_{\min}$, in the e^+e^- c.m. frame. The fragmentation function for a muon emitted from a photon can be obtained from (2.9) by the Gribov-Lipatov relation[13]

$$G_{\mu/\gamma}(x)=xG_{\gamma/\mu}\left(\frac{1}{x}\right)$$

$$=\frac{\alpha}{2\pi}\ln\left(\frac{s}{4m_\mu^2}\right)[x^2+(1-x)^2] \tag{2.10}$$

and the distribution for muons from an electron by convolution:

$$G_{\mu/e}(x)\cong\frac{\alpha}{2\pi}\ln\frac{s}{4m_e^2}\frac{\alpha}{2\pi}\ln\frac{s}{4m_\mu^2}\left(\frac{1-x}{x}\right). \tag{2.11}$$

If we could rely on only the Born diagrams in QCD, then the distribution of quarks in a photon would be given directly from (2.10)

$$G_{q/\gamma}^{\text{Born}}(x)=\frac{\alpha}{2\pi}e_q^2\ln\frac{s}{4M^2}[x^2+(1-x)^2] \tag{2.12}$$

for a quark of each color. We have assumed that the region of $k_T^2<M^2$, where $M\sim 0$ (300 MeV) is represented by a separate vector-meson contribution which we compute below.

As first shown by Witten,[4] the corrections to (2.12) due to gluon bremsstrahlung can be computed to all orders in α_c, keeping leading logarithms in each order. The simplest method is to use the convolution formula

$$G_{q/\gamma}(x,Q^2)=\frac{\alpha}{2\pi}e_q^2\int_{\sim M^2}^{Q^2}\frac{dk^2}{k^2}\int_x^1\frac{dz}{z}[z^2+(1-z)^2]$$

$$\times G_{q'/q}(x/z,Q^2,k^2), \tag{2.13}$$

where $G_{q'/q}(x,Q^2,k^2)$ is the distribution of quarks (at spacelike mass squared Q^2) in a quark (at mass squared k^2) allowing for gluon bremsstrahlung to all orders. To the accuracy required here it will be sufficient to only consider q' and q of the same flavor and disregard the $g\to q'\bar{q}'$ mixing terms. Also, to the leading-logarithmic accuracy we can identify $(k^2)_{\max}=Q^2=-sx/(1-x)$ with s. Using the moment analysis discussed in Appendix B, we find for asymptotic s

$$xG_{q/\gamma}(x,s)=\frac{\alpha}{2\pi}e_q^2\frac{f(x)}{\alpha_c(s)}, \tag{2.14}$$

which is to be summed over quark color and flavor. The scaling function $f(x)$ is plotted in Fig. 1(a) (see also Ref. 5). A comparison with the Born approximation (2.12) is also shown. When $1-x$ is small, we can use[15]

$$f(x)\cong\frac{4\pi}{4\pi b-(3-4\gamma_E)C_2+4C_2\ln[1/(1-x)]}, \tag{2.15}$$

where γ_E is Euler's constant, $C_2=(N^2-1)/2N=\frac{4}{3}$ for SU(3) color, and $4\pi b=(11-\frac{2}{3}n_f)\cong 9$ characterizes the asymptotic behavior of the running coupling constant, $\alpha_c(Q^2)\to 1/(b\ln Q^2/\Lambda^2)$. A comparison of $f(x)$ with the asymptotic form (2.15) is also shown in Fig. 1(a).

The convolution of $G_{q/\gamma}$ and $G_{\gamma/e}$ then gives for each quark of given color and flavor

$$xG_{q/e}(x,s)\cong\left(\frac{\alpha}{2\pi}\right)^2e_q^2\frac{\ln\eta}{\alpha_c(s)}(1-x)\tilde{f}(x), \tag{2.16}$$

where $\tilde{f}(x)$ is shown in Fig. 1(b). For $1-x$ small, $\tilde{f}(x)$ also has the limiting form described by (2.15).

A remarkable fact is that when we compute high-p_T jet cross sections at fixed $p_T/\sqrt{s}$ from the qq

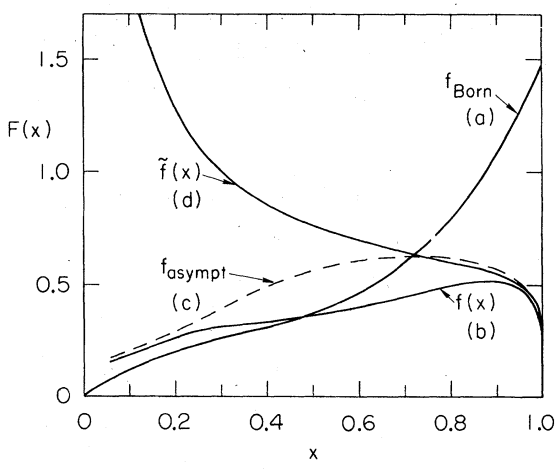

FIG. 1. The structure function of the photon $f(x)=xG_{q/\gamma}(x,Q^2)/[(\alpha/2\pi)e_q^2/\alpha_c(Q^2)]$, as computed in perturbative QCD, (a) the Born approximation from Eq. (2.12): $f_{\text{Born}}(x)=x[x^2+(1-x)^2]/b$. (b) The nonsinglet (valence) structure function $f(x)$ computed from QCD to all orders. See Eq. (2.14) and Appendix B. (c) The asymptotic form for $f(x)$ given in Eq. (2.15). (d) The structure function $\tilde{f}(x)$ for $G_{q/e}$ as defined in Eq. (2.16).

$\to qq$ and $\gamma q \to gq$ subprocesses using Eq. (2.3), the scale violation from the factors of α_c in the subprocess cross sections cancels to leading-logarithmic order the $1/\alpha_c$ factors in the q/γ distribution functions. Thus, aside from the logarithmic factors in the equivalent-photon approximation, the jet cross sections for the $\gamma\gamma$ process actually Bjorken-scale in the asymptotic limit.[14]

For the nonperturbative part of the photon structure functions, we shall use the vector-meson-dominance model. The distribution of virtual vector mesons in the electron is then given by

$$G_{V/e}(x) = \frac{4\pi\alpha}{f_V^2} G_{\gamma/e}(x), \tag{2.17}$$

where $f_\rho^2/4\pi = 2.2$ for the ρ. For the distribution of quarks in the meson we take the simple form $xG_{q/V}(x) = C_V(1-x)$ where $C_V = 0.5$ corresponds to each quark carrying $\frac{1}{4}$ of the total momentum. Then for each quark color and flavor

$$\sum_{q=u,d} xG_{q/e}^{\text{non-pert}}(x) \cong \frac{1}{3}\frac{\alpha^2}{f_V^2} C_V \ln\eta \times [(1-x)^2 + \tfrac{2}{3}(1-x)^3 + \cdots] . \tag{2.18}$$

(This should be summed over color and vector mesons when the total color and flavor contribution is required). The distributions (2.16) and (2.18) taken together should give a reasonably accurate representation of the effective quark distributions.

Finally, in order to obtain single-particle cross sections from subprocesses involving a large-transverse-momentum quark we need the probability of finding a meson in a quark. The fragmentation function for π^+'s out of quarks may be fitted from e^+e^- data.[16] Assuming $G_{\pi^+/u}(x) = G_{\pi^-/\bar{u}}(x) = G_{\pi^+/\bar{d}}(x) = G_{\pi^-/d}(x)$, a reasonable fit (though not a unique one) is

$$xG_{\pi^+/u}(x) = 0.5[(1-x) + (1-x)^3] , \tag{2.19}$$

although in general QCD scaling violations should be included.

TABLE I. Fragmentation functions,

$$xG_{a/A}(x) = \sum_i \Lambda_a^i (1+g_a^i)(1-x)^{g_a^i} .$$

All fragmentation functions are per color and for unit charge quarks, and are evaluated at $\sqrt{s} = 30$ GeV, with $f_\rho^2/4\pi = 2.2$, $\ln\eta = \ln(s/4m_e^2) = 20.4$.

A	a	$g_a^{(1)}$	$\Lambda_a^{(1)}$	$g_a^{(2)}$	$\Lambda_a^{(2)}$
e	γ	0	2.37×10^{-2}	2	0.79×10^{-2}
e	ρ	0	7.86×10^{-5}	2	2.62×10^{-5}
e	q	1	1.1×10^{-4}		
e	$(u+d)/\rho$	2	2.2×10^{-6}	3	1.1×10^{-6}
q	π	1	0.25		

In the calculations to be described below, we include only the $(1-x)$ piece of (2.19) and neglect all "unfavored" fragmentation [$G_{\pi^-/u}(x) = 0$, for instance]. All these fragmentation functions are tabulated in Table I.

C. Generic forms of reaction cross sections

Next we shall collect some approximate formulas which will be of help in estimating the sizes of various differential cross sections. Exact formulas and their derivation are given in Appendix A and in Refs. 7 and 17. (The calculations we show later on are the results of numerical integration over these exact formulas).

If we parametrize a fragmentation function as

$$xG_{a/A}(x) = (1+g_a)\Lambda_{a/A}(1-x)^{g_a} \tag{2.20}$$

and the differential cross section for the subprocess as

$$\frac{d\sigma}{dt} = \pi D s^{-(N-T-U)}(-t)^{-T}(-u)^{-U} , \tag{2.21}$$

then Eq. (2.3) reduces to

$$\frac{E\,d\sigma}{d^3p}(AB \to CX) = \frac{1}{s^N}\left(\frac{-t}{s}\right)^{-T}\left(\frac{-u}{s}\right)^{-U}(1+g_a)(1+g_b)\Lambda_{a/A}\Lambda_{b/B}D \times \int dx_1 dx_2 (1-x_1)^{g_a}(1-x_2)^{g_b}(x_1)^{U-N-1}(x_2)^{T-N-1}\delta\left(1+\frac{t}{sx_1}+\frac{u}{sx_2}\right) . \tag{2.22}$$

Now we write

$$x_R \equiv 1-\epsilon = 2|p^c|/\sqrt{s}\,,$$
$$x_F \equiv \frac{2p_\parallel^c}{\sqrt{s}}\,, \tag{2.23}$$
$$x_T = \frac{2p_T^c}{\sqrt{s}}\,,$$

so that

$$\frac{-t}{s} = \tfrac{1}{2}(1-\epsilon-x_F),\quad \frac{-u}{s} = \tfrac{1}{2}(1-\epsilon+x_F)\,, \tag{2.24}$$

and

$$s = \frac{4p_T^2}{x_T^2} = \frac{4p_T^2}{(1-\epsilon-x_F)(1-\epsilon+x_F)}\,. \tag{2.25}$$

We can then evaluate the integrals in (2.22) and write[2]

$$\frac{Ed\sigma}{d^3p}(AB\to CX) = \frac{D\epsilon^F}{(p_T^2)^N}\Lambda_{a/A}\Lambda_{b/B}2^{f_+ + f_-} \times \frac{\Gamma(2+g_a)\Gamma(2+g_b)}{\Gamma(2+g_a+g_b)} \times (1-\epsilon-x_F)^{-f_+}(1-\epsilon+x_F)^{-f_-}\tilde{J}\,, \tag{2.26}$$

where

$$F = 1+g_a+g_b\,,$$
$$f_+ = T+1+g_b-N\,, \tag{2.27}$$
$$f_- = U+1+g_a-N\,,$$

and

$$\tilde{J} = \frac{1}{J_0}\int_{-1}^{1} dw(1+w)^{g_a}(1-w)^{g_b}\left(\frac{1+x_F+\epsilon w}{1+x_F-\epsilon}\right)^{-f_-} \times \left(\frac{1-x_F-\epsilon w}{1-x_F-\epsilon}\right)^{-f_+}\,,$$
$$J_0 = \int_{-1}^{1} dw(1+w)^{g_a}(1-w)^{g_b}\,. \tag{2.28}$$

Similar expressions are obtained for the case of a final state fragmentation as well and are given in Appendix A.

These expressions are still an exact representation of Eq. (2.22), but the approximate evaluation of $\tilde{J}$ by its value at $\epsilon = 0$, $\tilde{J}(\epsilon = 0) = 1$, provides a useful approximation valid for small ϵ, near the edge of phase space.

D. Some counting factors

We must now face the task of enumerating all the different contributions to the jet or single-particle cross section. In order to facilitate matters, we will discuss some multiplicative factors which are common to all subprocesses. To do this, we define

$$F(a,b,d\sigma/dt) \equiv \int_0^1 dx_a dx_b G_{a/A}(x_a)G_{b/B}(x_b) \times \frac{d\hat{\sigma}}{d\hat{t}}\frac{\hat{s}}{\pi}\delta(\hat{s}+\hat{t}+\hat{u}) \tag{2.29}$$

and [see Eq. (A9)]

$$F(a,b,C,d\sigma/dt) \equiv \int_0^1 dx_a dx_b \frac{dx_c}{x_c^2} G_{a/A}(x_a)G_{b/B}(x_b)G_{C/c}(x_c)\frac{d\hat{\sigma}}{d\hat{t}}\frac{\hat{s}}{\pi}\delta(\hat{s}+\hat{t}+\hat{u})\,, \tag{2.30}$$

the "bare" convolution formulas for the differential cross sections. Multiplicative factors which we shall frequently encounter are as follows:

1. Beam-target symmetrization. A process in which the electron emits a parton of type (a) which scatters from a parton of type (b) emitted by the positron is as likely as a process in which "b" came from the electron and "a" from the positron. To include both these reactions, we introduce a symmetrized differential cross section

$$F_S\left(a,b,\frac{d\sigma}{dt}\right) = \frac{1}{2}\left[F\left(a,b,\frac{d\sigma}{dt}\right)+F\left(b,a,\frac{d\sigma}{du}\right)\right] \tag{2.31}$$

[and similarly for $F_S(a,b,c,d\sigma/dt)$] where if $d\sigma/dt = f(t,u)$, $d\sigma/du = f(u,t)$. Our normalization is such that if $a \neq b$, a given process will be weighted

by an additional factor of 2, which we will refer to in the next section as a "beam-target symmetrized factor."

2. In the case of jet cross sections, the jet can be either of the two groups of particles at large p_T. To include this we write a jet-symmetrized cross section

$$F_J\left(a,b,\frac{d\sigma}{dt}\right)=F\left(a,b,\frac{1}{2}\left(\frac{d\sigma}{dt}+\frac{d\sigma}{du}\right)\right) \tag{2.32}$$

(normalized so that jet cross sections are given by $2F_J$). We may combine jet and beam-target symmetrization to write

$$F_{SJ}\left(a,b,\frac{d\sigma}{dt}\right)=\left[\tfrac{1}{2}F\left(a,b,\frac{1}{2}\left(\frac{d\sigma}{dt}+\frac{d\sigma}{du}\right)\right)+F\left(b,a,\frac{1}{2}\left(\frac{d\sigma}{dt}+\frac{d\sigma}{du}\right)\right)\right]. \tag{2.33}$$

The total jet cross section is then given by $4F_{SJ}$.

3. Finally, we will show explicitly all color and charge factors, wave-function normalizations, and the like.

III. HARD-SCATTERING SUBPROCESSES FOR $\gamma\gamma$ COLLISIONS

The number of different scattering subprocesses which may, in principle, contribute to jet or single-particle production is large. To facilitate our discussion of them in a coherent way, we will classify them according to their p_T behavior at large p_T. It happens that all of the important subprocesses which we consider vary as p_T^{-N}, where $N=4$, 6, or 8. We discuss each of these classes separately in Secs. III A, III B, and III C.

A. p_T^{-4} subprocesses

These reactions exhibit the underlying structure of a scale-invariant pointlike coupling and from that standpoint are the most interesting and fundamental of any of the interactions which may be studied in $\gamma\gamma$ collisions.

1. $\gamma\gamma\to q\bar{q}$. The simplest reaction we may consider is shown in Fig. 2(a), the production of a single pion or a hadronic jet via quark fragmentation.[3] The subprocess cross section is

$$\frac{1}{2}\left(\frac{d\sigma}{dt}+\frac{d\sigma}{du}\right)=\frac{2\pi\alpha^2}{s^2}\left(\frac{t}{u}+\frac{u}{t}\right), \tag{3.1}$$

whence

$$\frac{Ed\sigma(\text{jet})}{d^3p}=2\times 3\sum_{i=ud sc} e_i^4 F_J\left(\gamma,\gamma,\frac{1}{2}\left(\frac{d\sigma}{dt}+\frac{d\sigma}{du}\right)\right), \tag{3.2}$$

$$\frac{Ed\sigma(\pi^+)}{d^3p}=3\sum_{i=u,\bar{d}} e_i^4 F\left(\gamma,\gamma,\pi,\frac{1}{2}\left(\frac{d\sigma}{dt}+\frac{d\sigma}{du}\right)\right). \tag{3.3}$$

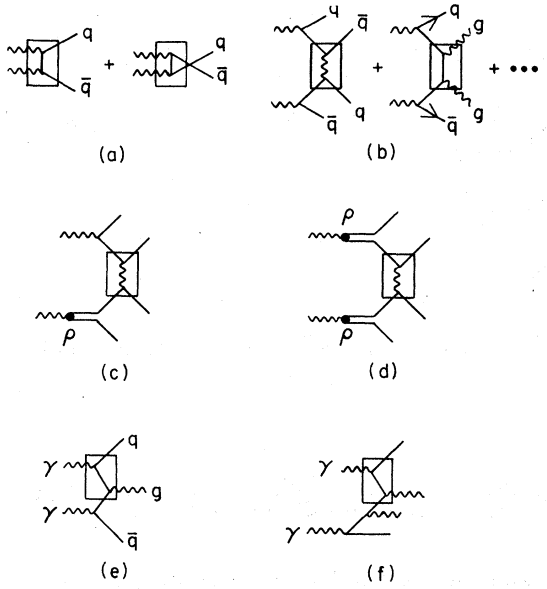

FIG. 2. Graphs for $\gamma\gamma$ inclusive cross sections proportional to p_T^{-4}. A box encloses the hard scattering. (a) $\gamma\gamma\to q\bar{q}$, (b) $\gamma\gamma\to q\bar{q}q\bar{q}$, $q\bar{q}gg$, (c) $\gamma\rho\to q\bar{q}q\bar{q}$, (d) $\rho\rho\to q\bar{q}q\bar{q}$, (e) $\gamma\gamma\to q\bar{q}g$, and (f) a radiative correction to the three-jet topology.

The factor of 2 is from jet symmetrization and the factor of 3 is from color. This reaction admits to a new constant of proportionality with relation to the reaction $e^+e^-\to e^+e^-\mu^+\mu^-$: Equation (3.2) implies

$$\frac{Ed\sigma}{d^3p}(e^+e^-\to e^+e^-\,\text{jet}\,X)=2R_{\gamma\gamma}\frac{Ed\sigma}{d^3p}(e^+e^-\to e^+e^-\mu^+\mu^-), \tag{3.4}$$

where

$$R_{\gamma\gamma}=3\sum_{i=udsc} e_i^4=\tfrac{34}{27}. \tag{3.5}$$

Evaluation of (3.2) and (3.3) yields the approximate forms

$$\frac{Ed\sigma(\text{jet})}{d^3p}\sim 0.03\,\frac{(1-x_R)}{p_T^4}\,\text{nb GeV}^2, \tag{3.6}$$

$$\frac{Ed\sigma(\pi^+)}{d^3p}\sim 6.3\times 10^{-4}\,\frac{(1-x_R)^3}{p_T^4}\,\text{nb GeV}^2 \tag{3.7}$$

at $\sqrt{s}=30$ GeV. These results are accurate for $x_R\to 1$ at all $\theta_{\text{c.m.}}$.

There will also be calculable corrections of order $\alpha_s(p_T^2)$ to $R_{\gamma\gamma}$ from higher QCD corrections to the $\gamma\gamma\to\text{jet}+X$ scaling cross sec-

tion. There are no corrections of order $\alpha_c(p_T^2)\ln p_T^2$ since

(a) infrared gluon-mass singularities cancel for the inclusive jet cross section, and

(b) there is no quark-mass singularity since the gluon corrections to the $\gamma\gamma \to q\bar{q}$ amplitude (not already canceled by renormalization terms) connect quark lines of different momentum. (This is a sufficient condition for absence of mass singularities if one uses an axial or Coulomb gauge.)

The perturbative corrections to $\gamma\gamma \to q\bar{q}$ are thus of the same form as that for $e^+e^- \to q\bar{q}$ and are expressible as a power series in $\alpha_c(p_T^2)$.[14]

The observation of a p_T^{-4} distribution in the jet or single-particle cross section will also be an important confirmation of the idea that the quark propagator has a $1/\not{p}$ component which may be seen at large momentum transfer—and the reaction $\gamma\gamma \to q\bar{q}$ may be the first one in which that part of the quark propagator will be clearly exposed.

The value of $R_{\gamma\gamma}$ given by Eq. (3.5) is an asymptotic form, as $\alpha_c(p_T^2)$ and $m_q^2/p_T^2 \to 0$. It will be interesting to study the approach of $R_{\gamma\gamma}$ from $3\sum_{i=uds} e_i^4$ to $3\sum_{i=udsc} e_i^4$ as a function of s and p_T.

2. $\gamma\gamma \to q\bar{q}q\bar{q}$. These reactions, shown in Fig. 2(b), involve explicit gluon exchange (or $q\bar{q}$ annihilation into gluons) as the source of the high-p_T events. They are four-jet events, since one of the quarks in each photon is a spectator to the large-p_T reaction and forms its own jet along the beam axis, following the photon's original line of motion.

TABLE II. QCD differential cross sections, summed over initial colors, have a generic form

$$\frac{d\sigma}{dt}(ij \to kl) = \frac{4\pi\alpha_c^2}{s^2}\Sigma,$$

where Σ is tabulated here.

$\Sigma(i = q_i \text{ or } \bar{q}_i, j = q_j \text{ or } \bar{q}_j, i \neq j)$	$\frac{s^2+u^2}{t^2}$
$\Sigma(q_iq_i \to q_iq_i \text{ or } \bar{q}_i\bar{q}_i \to \bar{q}_i\bar{q}_i)$	$\frac{s^2+u^2}{t^2} + \frac{s^2+t^2}{u^2} - \frac{2}{3}\frac{s^2}{tu}$
$\Sigma(q_i\bar{q}_i \to q_i\bar{q}_i)$	$\frac{s^2+u^2}{t^2} + \frac{t^2+u^2}{s^2} - \frac{2}{3}\frac{u^2}{st}$
$\Sigma(q_i\bar{q}_i \to q_j\bar{q}_j, i \neq j)$	$\frac{t^2+u^2}{s^2}$
$\Sigma(q_i\bar{q}_i \to gg)$	$\frac{8}{3}\left(\frac{t}{u}+\frac{u}{t}\right) - 6\left(\frac{t^2+u^2}{s^2}\right)$

The various subprocesses ($qq \to qq$, $q\bar{q} \to gg$, etc.) which are to be included in the large-p_T reaction have been computed by many authors[18] and it is most convenient to adapt their results to our needs. The various symmetrizations which must be performed make this a delicate process, however. For instance, a jet trigger occurs whenever one detects *any* high-p_T particle produced in the reaction. Thus, for jet triggers, one must (generally) include a particular subprocess plus the $t \rightleftarrows u$ crossed subprocess, corresponding to triggering on the other jet. For example, in $\gamma_1 \to q_1\bar{q}_1$, $\gamma_2 \to q_2\bar{q}_2$, followed by q_1q_2 scattering ($q_1 \neq q_2$), we compute $Ed\sigma/d^3p(e^+e^- \to q_1X)$ using the subprocess $d\sigma/dt(q_1q_2 \to q_1q_2)$ and add it to $Ed\sigma/d^3p(e^+e^- \to q_2X)$ using the subprocess $d\sigma/dt(q_1q_2 \to q_2q_1)$. If nonidentical particles scatter, one must also explicitly include cases $\gamma_1 \to q_2\bar{q}_2$ $+\gamma_2 \to q_1\bar{q}_1$ followed by q_2q_1 scattering. If identical particles scatter, however, one has already "included the crossed terms" in the full expression (including interference as required by quantum mechanics) for the scattering subprocess. Similarly for the π^+ spectrum, we assume that only a u or a $\bar{d}$ quark can fragment into a fast π^+. But the u ($\bar{d}$) quark may be produced via reactions where the u ($\bar{d}$) quark originates from γ_1 (say), $d\sigma/dt(e^+e^- \to u(\bar{d})X)$, or by the crossed reactions in which the u ($\bar{d}$) originates from γ_2, $d\sigma/du$ $(e^+e^- \to u(\bar{d})\bar{X})$. The relevant quark-quark scattering terms are shown in Table II.

After summing over all possible contributions (using the fact that all initial q's and $\bar{q}$'s from each photon γ_1 and γ_2 are equally likely) we may express our result in terms of an "effective" subprocess cross section

$$\frac{d\sigma}{dt}\left(\sum \text{all } q \text{ or } \bar{q} + \sum \text{all } q \text{ or } \bar{q} \to \text{any trigger } q \text{ or } \bar{q} + \text{balancing } q \text{ or } \bar{q}\right) \tag{3.8}$$

for jet production and

$$\frac{d\sigma}{dt}\left(\sum \text{all } q \text{ or } \bar{q} + \sum \text{all } q \text{ or } \bar{q} \to u(\bar{d}) + \text{balancing } q \text{ or } \bar{q}\right) \tag{3.9}$$

for π^+ production. These "subprocesses" include all crossing and other factors and are to be folded with the $G_{q/e}$ forms of Sec. II, where we again recall that $G_{q/e} = G_{\bar{q}/e}$ for all quark types to first approximation. The effective cross-section forms appear in Table III. The color sums are already included in these cross sections.

In order to obtain simple analytic expressions for the inclusive cross sections, let us first ap-

TABLE III. $\gamma\gamma \to q\bar{q}q\bar{q}$ jet and π^+ effective cross sections. The cross sections are summed (but not averaged) over color.

$$\frac{d\sigma^{\text{jet}}}{dt}(qq+q\bar{q}+\bar{q}q+\bar{q}\bar{q}\to\text{final-state quarks or antiquarks})$$

$$=\frac{4\pi\alpha_c^2}{s^2}\left\{\left[\frac{s^2+u^2}{t^2}+\frac{s^2+t^2}{u^2}\right]4\left(\sum e_i^2\right)^2+\left[\frac{t^2+u^2}{s^2}N_f-\frac{1}{3}\left(\frac{s^2}{tu}+\frac{t^2}{su}+\frac{u^2}{st}\right)\right]4\sum e_i^4\right\},$$

N_f = number of quark flavors

$$\frac{d\sigma^{\text{jet}}}{dt}(q\bar{q}\to\text{final-state gluons})=\frac{4\pi\alpha_c^2}{s^2}\left[\frac{8}{3}\left(\frac{t}{u}+\frac{u}{t}\right)-6\left(\frac{t^2+u^2}{s^2}\right)\right]2\sum e_i^4$$

$$\frac{d\sigma^{\pi^+}}{dt}(qq+q\bar{q}+\bar{q}q+\bar{q}\bar{q}\to uX \text{ or } \bar{d}X)$$

$$=\frac{4\pi\alpha_c^2}{s^2}\left[2\left(\sum_{i=u,\bar{d}}e_i^2\right)\left(\sum_{j=u\,d\,s\,c}e_j^2\right)\left(\frac{s^2+u^2}{t^2}+\frac{s^2+t^2}{u^2}\right)\right.$$
$$\left.+4\sum_{i=u\,d\,s\,c}e_i^4\left(\frac{t^2+u^2}{s^2}\right)+\sum_{i=u,d}e_i^4\left(-\frac{2}{3}\right)\left(\frac{s^2}{tu}+\frac{t^2}{su}+\frac{u^2}{st}\right)\right]$$

proximate $G_{q/e}$ in Eq. (2.16) by the simple form

$$xG_{q/e}(x)=e_q^2\left(\frac{\alpha}{2\pi}\ln\eta\right)\left(\frac{\alpha}{2\pi}F_Q\right)(1-x) \qquad (3.10)$$

for each quark flavor and color, where roughly $F_Q\cong\ln s/4M_q^2$ if we use the simple Born graphs for $\gamma\to q\bar{q}$, and $F_Q\cong[1/\alpha_c(s)]\langle\tilde{f}(x)\rangle$ if we use the full QCD result. For a rough estimate we shall take $\alpha_c(p_T^2)\times F_Q\cong 1.2$. The vector-meson-dominated contributions will be considered separately.

Using (3.10) we then find

$$\frac{Ed\sigma}{d^3p}(e^+e^-\to e^+e^-+\text{jet}+X)=F_J\left(q,q,\frac{d\sigma^{\text{eff}}}{dt}\right)$$

$$\simeq\alpha_c^2(p_T^2)\left(\frac{\alpha}{2\pi}\ln\eta\right)^2\left(\frac{\alpha}{2\pi}F_Q\right)^2\left[\frac{80}{3}\left(\sum_{i=u\,d\,s\,c}e_i^2\right)^2+\frac{52}{9}\sum_{i=u\,d\,s\,c}e_i^4\right]\frac{(1-x_R)^3}{p_T^4}\ \text{GeV}^4$$

$$\underset{\theta_{\text{c.m.}}=90}{\overset{x_R\to 1}{\sim}}\ 1.7\times10^{-2}(1-x_R)^3p_T^{-4}\ \text{nb GeV}^2, \qquad (3.11)$$

$$\frac{Ed\sigma}{d^3p}(e^+e^-\to e^+e^-\pi^+X)=F\left(q,q,\pi,\frac{d\sigma^{\text{eff}}}{dt}\right)\underset{\theta_{\text{c.m.}}=90}{\overset{x_R\to 1}{\sim}}\ 1.3\times10^{-4}\frac{(1-x_R)^5}{p_T^4}\ \text{nb GeV}^2 \qquad (3.12)$$

at $\sqrt{s}=30$ GeV. The charge structures of the various contributing terms are displayed in Eq. (3.11). The numerical coefficients in (3.11) and (3.12) are the result of a numerical integration of Eq. (2.3). Equations (3.11) and (3.12) are useful as phenomenological approximations in that they display the approximate analytic and quark charge dependence of the inclusive cross sections.

We have also directly computed the $e^+e^-\to e^+e^-$ +jet+X cross section from (2.25) using the full QCD form (2.16) for the quark distribution in the electron $G_{q/e}(x,s)$, allowing for gluon brems-

strahlung to all orders. Again we note the asymptotic cancellation of the $\alpha_c^2(p_T^2)$ factor from $d\sigma/dt(qq \to qq)$ and the $\alpha_c^{-1}(p_T^2)$ factors in $G_{q/e}(x,s)$ at fixed x_T.

The resulting (four-jet) cross section has the asymptotic scaling form

$$\frac{Ed\sigma}{d^3p}(ee \to \text{jet} + X) = \frac{\left(\frac{\alpha}{\pi}\ln\eta\right)^2}{p_T^2} \times \left[f(x_T, \theta_{\text{c.m.}}) + O\left(\frac{1}{\ln p_T^2}\right)\right]. \tag{3.13}$$

A comparison of cross sections using the full QCD and Born contributions for $G_{q/e}$ and specific results for PETRA and PEP energies are given in Sec. IV.

3. *$\gamma p \to q\bar{q}q\bar{q}$ and $pp \to q\bar{q}q\bar{q}$ [Figs. 2(c)–2(d)].* The latter vector-dominance contribution is the $\gamma\gamma$ analog of pp scattering mediated by gluon exchange.[19] It is quite small with respect to either $\gamma\gamma \to q\bar{q}$ or $\gamma\gamma \to q\bar{q}q\bar{q}$ perturbative contributions, the change in size being due mainly to the small probability for the sequential transition $\gamma \to \rho \to q\bar{q}$. We can obtain an estimate of the contribution by considering only qq scattering via gluon exchange (this neglects the small identical-particle and annihilation effects)

$$\frac{d\sigma}{dt} = \frac{4\pi}{9}\alpha_c^2\left(\frac{s^2+u^2}{t^2}\right), \tag{3.14}$$

whence

$$\frac{Ed\sigma(\text{jet})}{d^3p} = (\tfrac{1}{2}\times 4)^2 \times 3^2 \times 2F_J\left(q/\rho, q/\rho, \frac{d\sigma}{dt}\right) \simeq 1.1\times 10^{-5}\,\frac{(1-x_R)^5}{p_T^4}\ \text{nb GeV}^2 \tag{3.15}$$

at $\sqrt{s} = 30$ GeV, $\theta_{\text{c.m.}} = 90°$, $1 - x_R$ small. The 3's are color traces and 4's and $\frac{1}{2}$'s the meson flavor sums and wave-function normalizations. The inclusive π^+ cross section is also quite small.

The $\gamma p \to q\bar{q}q\bar{q}$ cross sections are somewhat larger. Using the same technique [i.e., neglecting small identical particle and annihilation contributions by using Eq. (3.14)], we have

$$\frac{Ed\sigma(\text{jet})}{d^3p} = (\tfrac{1}{2}\times 4)\left[3^2\times 2\sum_{i=udsc} e_i^2(4)\right] \times F_{JS}\left(q/e, q/\rho, \frac{d\sigma}{dt}\right) \tag{3.16}$$

$$= 4.6\times 10^{-4}\,\frac{(1-x_R)^4}{p_T^4}\ \text{nb GeV}^2 \tag{3.17}$$

at $\sqrt{s} = 30$ GeV, $\theta_{\text{c.m.}} = 90°$, small $1 - x_R$. The $\frac{1}{2}\times 4$ corresponds to the ρ wave-function factor and 4 flavor choices; the 3^2 is the sum over colors of colliding quarks; the $2\sum e_i^2$ is the choice of any q or $\bar{q}$ from the photon distribution; the 4 is the standard jet beam-target symmetrization. The result is less than 3% of the perturbative $\gamma\gamma \to q\bar{q}q\bar{q}$ contribution and thus is also negligible. One might also consider interference between, say, $\gamma\rho \to q\bar{q}q\bar{q}$ and $\gamma\gamma \to q\bar{q}q\bar{q}$; this corresponds to a nondiagonal quark distribution function where in the sqaure, the scattering quark arises from a ρ but is reabsorbed by a γ. Inclusion of such diagrams corresponds to off-diagonal VDM in that it presumes overlap of the low-mass ρ region with the high-mass bare region corresponding to high-mass vector mesons. We neglect this possibility. Note that we have implicitly assumed that it is not necessary to include explicitly the contributions of massive vector mesons as these are to a great extent already included in the perturbative contribution.

4. *Other p_T^{-4} reactions.* In addition to the subprocesses of Sec. III A 1–3, one may consider more complicated QCD processes. These processes may be categorized into two classes. First one may consider radiative corrections to already calculated processes. If QCD perturbation-theory calculations have any meaning, higher-order in α_c contributions to cross sections which have the same topological (number of jets produced) and charge structure will not appreciably alter the size and shape of the lowest-order cross section.

We must, however, consider higher-order in α_c contributions when they lead to configurations with a topology different from that of lower-order results. An example of this criterion is the inclusion of the α_c^2 four-jet events of Sec. III A 2. Another example of a new contribution is the $O(\alpha_c)$ process of Fig. 2(c), $\gamma\gamma \to q\bar{q}g$, where we require that the hard scattering be $\gamma q \to gq$. These events have $n_J = 3$, one of the large-p_T jets being a gluon jet. We find, using (3.10),

$$\frac{Ed\sigma}{d^3p}(e^+e^- \to e^+e^- + \text{jet} + X) = 3\times 4\times 2\times F_{SJ}\left(\gamma, q, \frac{8}{3}e_q^2\frac{\pi\alpha\alpha_c}{s^2}\left(\frac{t}{s}+\frac{s}{t}\right)\right) \tag{3.18}$$

$$\simeq \alpha_c\alpha\left(\frac{\alpha}{2\pi}\ln\eta\right)^2\frac{\alpha}{2\pi}F_Q\,\frac{(1-x_R)^2}{p_T^4}\sum e_i^4(40) \cong 0.038\ \text{nb GeV}^2\,\frac{(1-x_R)^2}{p_T^4} \tag{3.19}$$

at $\sqrt{s}=30$ GeV $\theta_{c.m.}=90°$ and $1-x_R$ small. In (3.18) in addition to the factor of 3 for color, one factor of 4 is the standard total jet factor (including beam-target symmetrization) and the factor of 2 counts $\gamma q \to gq + \gamma\bar{q} \to g\bar{q}$. This rate is $O(1-x_R)(\alpha_c/\pi)F_Q$ times the rate for $\gamma\gamma \to q\bar{q}$.

We also have computed the $\gamma q \to gq$ subprocess contribution to the three-jet cross section using the full QCD structure $G_{q/e}(x,s)$ given in (2.16). In the asymptotic limit the factor of $\alpha_c(p_T^2)$ in $d\sigma/dt(\gamma q \to gq)$ is canceled by the $\alpha_s^{-1}(s)$ in $G_{q/e}$, and asymptotic scale invariance at fixed x_T is again obtained for the $\gamma\gamma \to$ jet $+X$ cross section. A comparison of the Born term calculation and the full QCD contributions to $ee \to$ jet $+X$ at PETRA and PEP energies is given in Sec. IV.

Finally, we note that digrams such as that of Fig. 2(f) where the hard subprocess is $\gamma q \to gq$ and the other gluon is at low transverse momentum relative to the $\bar{q}$ spectrum are already included in our calculations when the full QCD structure function (2.16) is used.

B. p_T^{-6} reactions

We now turn to classes of reactions in which the underlying pointlike constituents of the initial or final state particles are not completely exposed. Such reactions should not be expected to exhibit canonical p_T^{-4} scaling.

We analyze such reactions from the standpoint of the constituent-interchange model (CIM).[7,9] This approach has the advantage that it allows us to normalize the magnitude of these nonscaling contributions via comparison with cross sections measured in inclusive and exclusive hadron-hadron large-p_T reactions (where the CIM has been shown to provide a consistent parametrization of the data for $p_T<8$ GeV). At this stage it is also worth pointing out that it is not inconsistent to include both QCD and CIM contributions; the CIM is contained within QCD on the level of internal bound-state systems which participate in subprocesses within the reaction and can be identified as "higher-twist" QCD contributions. The normalization of CIM processes is related to the analysis of Bethe-Salpeter wave functions at short distances in QCD, and is determined empirically from elastic large-p_T cross sections.[7,9]

The CIM contributions of importance here naturally divide themselves into two classes: those in which $Ed\sigma/d^3p \propto p_T^{-6}$, where either one photon vector-dominates or where the final-state hard scattering involves the production of one hadronic resonance at large p_T, and those in which $Ed\sigma/d^3p \propto p_T^{-8}$, where both photons vector-dominate before scattering or several resonances at large p_T are produced, or some combination of processes occurs.

We discuss first the p_T^{-6} subprocesses. As we noted in the Introduction, the p_T^{-6} contributions are distinctive features of photon-induced processes predicted by the CIM. Their observation at the levels we calculate below would provide important confirmation of the CIM. The existence of such unique contributions for processes involving photons is supported by model calculations in two-dimensional QCD. Backward scattering in cases where Regge exchanges are absent provides a two-dimensional analog of wide-angle scattering, and it was found that meson-meson elastic scattering decreases with a power very similar to that predicted by the CIM ($A \propto s^{-2}$) (slight modification for light mesons of the integral power law was found due to confinement).[20] We have studied photon + photon $\to$ meson + meson in this model and find again a power very similar to that predicted by the CIM due to the elementary nature of the photon, but again with slight modifications for light mesons due to confinement.

Here the relevant subprocess is $\gamma q \to Mg$, where M is a pseudoscalar-meson resonance. With the direction of particle flow as indicated in Fig. 3(a), one finds[7,17] using the minimally connected Born diagrams in QCD

$$\frac{d\sigma}{dt}(\gamma q \to Mq) = \pi\alpha\left(\frac{1}{3}\frac{g^2}{4\pi}\right)\frac{s^2+u^2}{t}A\,,$$
$$A = \left(\frac{e_i}{u} - \frac{e_j}{s}\right)^2. \tag{3.20}$$

No wave function or color sums have been performed. e_i and e_j are defined in Fig. 3. $\frac{1}{3}g^2/4\pi$ is the CIM $q\bar{q}M$ coupling constant α_M which has been determined phenomenologically[7] to be ~ 2 GeV^2. We will treat the production of a pseudoscalar M as the spin-averaged rate for production of a vector meson of the same flavor assignment.

To compute $\gamma p \to q\bar{q}$ we cross (3.20) and find [Fig. 3(b)]

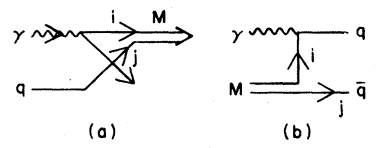

FIG. 3. The subprocesses which generate p_T^{-6} cross sections. The arrows on the labeled quark lines denote the direction of flow from which the quark's charge is to be read off.

$$\frac{d\sigma}{dt}(\gamma\rho \to q\bar{q}) = 2\pi\alpha\left(\frac{1}{3}\frac{g^2}{4\pi}\right)\frac{t^2+u^2}{s}\left(\frac{e_i}{t}-\frac{e_j}{u}\right)^2. \tag{3.21}$$

The factor of 2 converts an average over the spin of quark j into a sum.

We have found three important types of p_T^{-6} events:

1. $\gamma\rho \to q\bar{q}$ [*Fig.* 4(*a*)]. There is a finite probability that one photon will vector-dominate and that the other photon will scatter off the quarks in the bound-state wave function of the ρ. Of course, these events form two hadronic jets. The jet cross section is

$$\frac{Ed\sigma(\text{jet})}{d^3p} = 2\times\tfrac{1}{2}\times 3\times 2\sum_{i=u,\bar{d}} e_i^2 F_{JS}\left(\rho,\gamma,\frac{d\sigma}{dt}\right) \tag{3.22}$$

with

$$\frac{d\sigma}{dt} = 2\pi\alpha\left(\frac{1}{3}\frac{g^2}{4\pi}\right)\frac{t^2+u^2}{s^3}\left(\frac{1}{t}+\frac{1}{u}\right)^2. \tag{3.23}$$

In Eq. (3.22) one factor of 2 is for $\gamma\rho$ vs $\rho\gamma$ scattering, the other for triggering on either q or $\bar{q}$ jet (no third factor of 2 for q or $\bar{q}$ exchange since both pieces are included in the gauge-invariant cross section). There is also a factor of $\frac{1}{2}$ for the ρ wave function, and a factor of 3 for the color sum. Similarly, the single π^+ cross section is

$$\frac{Ed\sigma(\pi^+)}{d^3p} = 2\times\tfrac{1}{2}\times 3\sum_{i=u,\bar{d}} e_i^2 F_S\left(\rho,\gamma,\pi^+,\frac{d\sigma}{dt}\right) \tag{3.24}$$

with $d\sigma/dt$ given above. At $\sqrt{s}=30$ GeV, $\theta_{\text{c.m.}}=90°$, we obtain

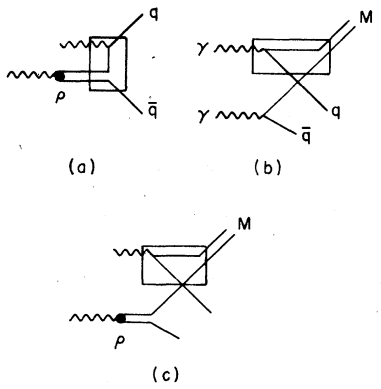

FIG. 4. Diagrams for p_T^{-6} inclusive cross sections (a) $\gamma\rho \to q\bar{q}$, (b) $\gamma\gamma \to Mq\bar{q}$, (c) $\gamma\rho \to Mq\bar{q}$.

$$\frac{Ed\sigma(\text{jet})}{d^3p} \sim 4.5\times 10^{-2}\,\frac{(1-x_R)}{p_T^6}\ \text{nb GeV}^4, \tag{3.25}$$

$$\frac{Ed\sigma(\pi^+)}{d^3p} \sim 1.06\times 10^{-3}\,\frac{(1-x_R)^3}{p_T^6}\ \text{nb GeV}^4. \tag{3.26}$$

At this point one must also note the possibility of interference between the processes $\gamma\gamma \to q\bar{q}$ and $\gamma\rho \to q\bar{q}$ since both have identical jet structure (including quantum numbers for a given $q\bar{q}$ choice). We have not explicitly calculated this interference but expect it is close to being maximal. Thus we estimate

$$\frac{Ed\sigma^{\text{interference}}(\text{jet})}{d^3p} = \left[\frac{Ed\sigma(\gamma\gamma)}{d^3p}\,\frac{Ed\sigma(\gamma\rho)}{d^3p}\right]^{1/2} \approx \frac{0.036}{p_T^5}(1-x_R)\ \text{nb GeV}^3. \tag{3.27}$$

Hence

$$\frac{\dfrac{Ed\sigma^{\text{interference}}(\text{jet})}{d^3p}}{\dfrac{Ed\sigma^{\gamma\gamma}(\text{jet})}{d^3p}} = \frac{1.2}{p_T}\ \text{GeV} \tag{3.28}$$

or approximately 30% at $p_T=4$ GeV. It will turn out that the third interfering process (p_T^{-8}) $\rho\rho - q\bar{q}$ is sufficiently small that we need not even consider its interference with those larger amplitudes.

2. $\gamma\gamma \to Mq\bar{q}$ [*Fig.* 4(*b*)]. This is a reaction with $n_J=3$, one jet being a meson resonance. To calculate the jet cross section, we sum over all q_i and $\bar{q}_j$ (or $\bar{q}_i$ and q_j) to find (including charge factors for both the bremsstrahlung and interacting M quark)

$$\frac{d\sigma}{dt} = \pi\alpha\left(\frac{1}{3}\frac{g^2}{4\pi}\right)\frac{s^2+u^2}{s^2t}\left(\frac{8}{9}\frac{1}{u^2}+\frac{4}{3}\frac{1}{s^2}\right), \tag{3.29}$$

which neglects charm-containing mesons

$$\frac{Ed\sigma(\text{jet})}{d^3p} = 3\times 4\times 4F_{JS}\left(\gamma,q,\frac{d\sigma}{dt}\right) = 1.1\,\frac{(1-x_R)^2}{p_T^6}\ \text{nb GeV}^4 \tag{3.30}$$

at $\sqrt{s}=30$ GeV, $\theta_{\text{c.m.}}=90°$. One factor of 4 is a beam target + either jet symmetrization, the factor of 3 is from the color sum, and the other factor of 4 is due to the spin sum over M. The sum over all quarks and their spins is equivalent to allowing the whole 35 + 1 of pseudoscalar and vector mesons to contribute to M. The π^+ cross section is found to be

$$\frac{E d\sigma(\text{prompt } \pi^+)}{d^3p} = 2\times 3F_S\left(\gamma, q, \frac{d\sigma}{dt}\right) \sim 0.031\frac{(1-x_R)^2}{p_T^{\,6}}\ \text{nb GeV}^2 \tag{3.31}$$

with

$$\frac{d\sigma}{dt} = \frac{\pi\alpha}{81}\left(\frac{1}{3}\frac{g^2}{4\pi}\right)\frac{s^2+u^2}{s^2t}\left(\frac{8}{u^2} - \frac{20}{us} + \frac{17}{s^2}\right). \tag{3.32}$$

Inclusion of "nonprompt" π's from resonance decays can double this answer.

3. $\gamma\rho \to Mq\bar{q}$. Finally, one photon may vector-dominate, decay into quarks, and scatter from the other photon [Fig. 4(c)]. The calculation is identical to Sec. III B 2 except for the ρ wave function and different charge structure.

For jets (neglecting charm-meson production) we have

$$\frac{d\sigma}{dt} = \pi\alpha\left(\frac{1}{3}\frac{g^2}{4\pi}\right)\frac{s^2+u^2}{s^2t}\frac{2}{3}\left(\frac{4}{u^2}+\frac{5}{s^2}\right),$$

$$\frac{E d\sigma(\text{jet})}{d^3p} = 4\times 4\times 3F_{JS}\left(\gamma, q/\rho, \frac{d\sigma}{dt}\right) = 0.13\frac{(1-x_R)^3}{p_T^{\,6}}\ \text{nb GeV}^4\ . \tag{3.34}$$

For π^+'s

$$\frac{d\sigma}{dt} = \tfrac{1}{9}\pi\alpha\left(\frac{1}{3}\frac{g^2}{4\pi}\right)\frac{s^2+u^2}{s^2t}\left(\frac{5}{u^2} - \frac{8}{us} + \frac{5}{s^2}\right), \tag{3.35}$$

$$\frac{E d\sigma(\text{prompt}\pi^+)}{d^3p} = 0.0051\frac{(1-x_R)^3}{p_T^{\,6}}\ \text{nb GeV}^4. \tag{3.36}$$

These p_T^{-6} processes $\gamma\gamma \to Mq\bar{q}$ and $\gamma\rho \to Mq\bar{q}$ again do not interfere in our diagonal approximation in which there is no overlap between distribution function quarks coming from a ρ versus the bare γ. Without such interference it is clear that the $\gamma\rho$ contributions are of order 10% of the $\gamma\gamma$ p_T^{-6} contribution.

C. p_T^{-8} contributions

Finally, we turn to the class of large-p_T scatterings which most nearly resemble those of purely hadronic reactions. The relevant cross section is that for quark-meson scattering, as displayed in Fig. 5.

1. $\rho\rho \to q\bar{q}$ [*Fig. 5(a)*]. Both photons may vector-dominate before scattering via quark exchange,

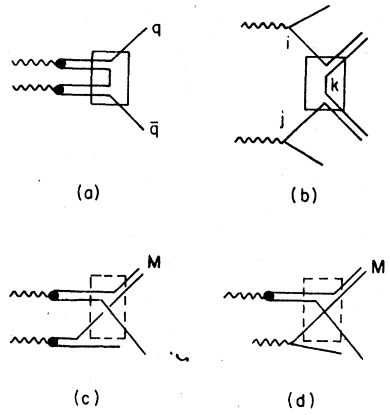

FIG. 5. Diagrams for p_T^{-8} inclusive cross sections (a) $\rho\rho \to q\bar{q}$, (b) $\gamma\gamma \to q\bar{q}M\bar{M}$, (c) $\rho\rho \to Mq\bar{q}$, (d) $\gamma\rho \to Mq\bar{q}$.

$$\frac{E d\sigma(\text{jet})}{d^3p} = 3\times 2\times(\tfrac{1}{2})^2\times 2\times 2\times F_J\left(\rho,\rho, 2\left(\frac{1}{3}\frac{g^2}{4\pi}\right)^2\frac{u}{s^2t^3}\right), \tag{3.37}$$

which is valid neglecting interference effects. One factor of 3 in (3.37) is from the color trace; one factor of 2 corresponds to looking at either the q or $\bar{q}$ jet; one factor of 2 is a flavor sum (u or d exchange; one factor of 2 for q or $\bar{q}$ exchange; and factors of $\frac{1}{2}$ for each ρ wave function)

$$\frac{E d\sigma(\text{jet})}{d^3p} \simeq 2_{\text{coh}}\times 10^{-2}\frac{(1-x_R)}{p_T^{\,8}}\ \text{nb-GeV}^6. \tag{3.38}$$

The extra factor 2_{coh} comes from the fact that there are really two coherently adding amplitudes in the $\rho\rho \to q\bar{q}$ cross section (as in Compton $\gamma\gamma \to q\bar{q}$). At 90° the net result is an increase of (3.37) by a factor of 2.

The π^+ cross section is given by a similar formula, except that no flavor sum on the exchanged quark is allowed, and (as in $\gamma\gamma \to q\bar{q}$), $d\sigma/du$ must be included to make sure that the "away" quark can fragment into a π:

$$\frac{E d\sigma}{d^3p} = 3.9\times\ 10^{-4}\times 2_{\text{coh}}\ \frac{(1-x_R)^3}{p_T^{\,8}}\ \text{nb GeV}^6. \tag{3.39}$$

Since these contributions are so very small compared to $\gamma\gamma \to q\bar{q}$ their interference with the latter is also negligible.

2. $\gamma\gamma \to q\bar{q}M\bar{M}$ [*Fig. 5(b)*]. Here the quarks scatter into meson jets in the final state. Two addi-

tional jets along the beam directions also accompany these large-p_T jets. We must sum over flavors u, d, s on quark (antiquark) i and over antiquark (quark) j:

$$\frac{E\,d\sigma(\text{jet})}{d^3p} 2\times 2\left(\sum_{i=uds} e_i\right)^2 3\times 3SF_{JS}\left(q,q,\frac{d\sigma}{dt}\right), \tag{3.40}$$

$$\frac{Ed\sigma(\text{prompt}\,\pi^+)}{d^3p} = 2\left(e_u{}^2+e_d{}^2\right)\left(\sum_{uds} e_j{}^2\right) \times 3S' F_S\left(q,q,\frac{d\sigma}{dt}+\frac{d\sigma}{du}\right). \tag{3.41}$$

In the jet cross section (3.40), one factor of 2 counts $q_i\bar{q}_j+q_i\bar{q}_j$, another factor of 2 is for observing a meson or quark jet, one factor of 3 is from a flavor sum over k, and S (S') are spin sums over i, j, and k. The easiest way to compute S and S' is to simply count 2 spin states per quark: $S=8$ and $S'=4$ (since in that case two spins are constrained to be antiparallel for π^+ production). At $\theta_{\text{c.m.}}=90°$, $1-x_R$ small,

$$\frac{E\,d\sigma(\text{jet})}{d^3p} = 0.24\,\frac{(1-x_R)^3}{p_T{}^8}\ \text{nb GeV}^6,$$

$$\frac{E\,d\sigma(\text{prompt}\ \pi^+)}{d^3p} = 1.7\times 10^{-2}\,\frac{(1-x_R)^3}{p_T{}^8}\ \text{nb GeV}^6. \tag{3.42}$$

3. $pp\to Mq\bar{q}$ [*Fig. 5(c)*]. This reaction is the one which is most similar to the processes which occur in $pp\to\pi X$. Both u- and s-channel quark exchange are possible: Counting flavors, one finds

$$\frac{d\sigma(\text{jet})}{dt} = 8\times(u\text{-channel exchange}) + 12\times(s\text{-channel exchange}),$$

$$\frac{d\sigma(\pi^+)}{dt} = 2\times(u\text{-channel exchange}) + 2\times(s\text{-channel exchange}), \tag{3.43}$$

where $d\sigma/dt\ (qM\to qM)=\pi\alpha_M{}^2/su^3$ for the u-channel exchange diagram, whence

$$\frac{E\,d\sigma(\text{jet})}{d^3p} = 4\times\left(\tfrac{1}{2}\right)^2\times 3\times 4F_{JS}\left(\rho,q/\rho,\frac{d\sigma}{dt}\right) \simeq 1.63\times 10^{-2}\,\frac{(1-x_R)^3}{p_T{}^8}\ \text{nb GeV}^6, \tag{3.44}$$

where the factor of 4 is a beam-target jet-symmetrization factor, the factor of $(\frac{1}{2})^2$ is from the ρ wave function, the factor of 3 is from the color trace, and the factor of 4 is due to a spin sum:

$$\frac{E\,d\sigma(\text{prompt}\,\pi^+)}{d^3p} = 2\times\left(\tfrac{1}{2}\right)^2\times 3F_S\left(\rho,q/\rho,\frac{d\sigma}{dt}\right) = 6.7\times 10^{-4}\,\frac{(1-x_R)^3}{p_T{}^8}\ \text{nb GeV}^6. \tag{3.45}$$

These reactions produce three jets, two at large p_T and a third along the beam direction. Both cross sections are much smaller than, and do not interfere (in the distribution function diagonal approximation) with, the following $\rho\gamma\to Mq\bar{q}$ contributions. In each case we take

$$\alpha_M\equiv\tfrac{1}{3}g^2/4\pi=2\ \text{GeV}^2.$$

4. $\rho\gamma\to Mq\bar{q}$ [*Fig. 5(d)*]. The Feynman graph for this process is identical to that for the reaction of Fig. 4(c). However, we assume that the hard scattering takes place in a different place in the graph from in that reaction. If we are to follow the precepts of the hard-scattering expansion we must include this contribution in addition to the former one. It is the sum over all hard scatterings which saturates the Feynman graph.

The calculation is similar to that for the contribution just shown above. We find

$$\frac{d\sigma(\text{jet})}{dt} = 4\sum_{i=u,\bar{d},s} e_i{}^2\ (u\text{-channel exchange}) + 6\sum_{i=u,\bar{d}} e_i{}^2\ (s\text{-channel exchange}),$$

$$\frac{d\sigma(\pi^+)}{dt} = \sum_{i=u,\bar{d}} e_i{}^2(u\text{-channel exchange} + s\text{-channel exchange}), \tag{3.46}$$

$$\frac{E\,d\sigma(q\ \text{or}\ M\,\text{jet})}{d^3p} = 4\times\left(\tfrac{1}{2}\right)\times 3\times 4\ F_{JS}\left(\rho,q,\frac{d\sigma}{dt}\right) = 0.18\,\frac{(1-x_R)^2}{p_T{}^8}\ \text{nb GeV}^6, \tag{3.47}$$

$$\frac{E\,d\sigma(\text{prompt}\ \pi^+)}{d^3p} = 2\times\left(\tfrac{1}{2}\right)\times 3F_S\left(\rho,q,\frac{d\sigma}{dt}\right) = 7.2\times 10^{-3}\,\frac{(1-x_R)^2}{p_T{}^8}\ \text{nb GeV}^6, \tag{3.48}$$

where the factor in (3.47) 4 is a beam-target jet-symmetrization factor, the factor of $\frac{1}{2}$ is from the wave-function normalization, the factor of 3 is a color trace, and the factor of 4 is from a spin sum.

This contribution, though it has the same Feynman-graph structure as the p_T^{-6} $\gamma\rho \to Mq\bar{q}$ contribution of Fig. 4(c), does not interfere with the latter in the diagonal-distribution-function approximation. However, it does interfere with the p_T^{-6} subprocess $\gamma\gamma \to Mq\bar{q}$. The interference is not quite maximal but we may obtain an upper bound by using maximal interference:

$$\frac{E\,d\sigma(\text{jet interference})}{d^3p} = 0.5\,\frac{(1-x_R)^2}{p_T^{\,7}}\ \text{nb GeV}^5 \tag{3.49}$$

or

$$\frac{E\,d\sigma(\text{interference})}{\dfrac{d^3p}{E\,d\sigma(\gamma\gamma \to Mq\bar{q})}} = \frac{0.5}{p_T}\ \text{GeV}\,, \tag{3.50}$$
$$\frac{d^3p}{}$$

which is small.

IV. RESULTS

As we have discussed in Sec. III, there are many contributions to jet and single-particle production in $\gamma\gamma$ collisions, even though this is per-

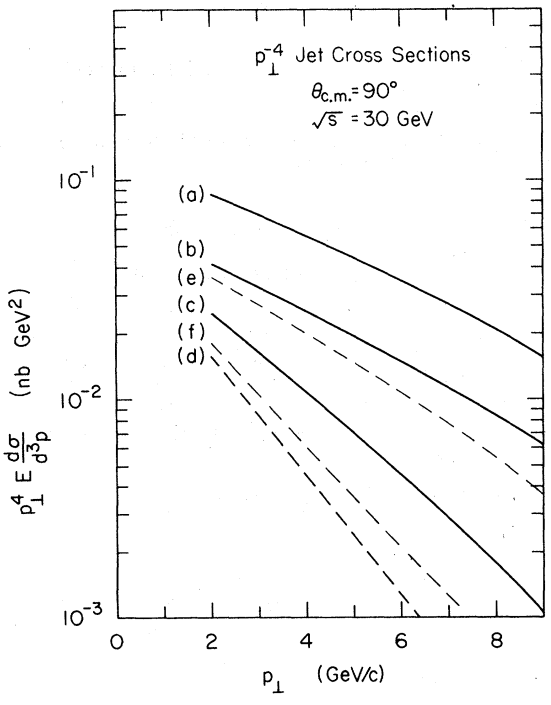

FIG. 6. Inclusive jet cross sections which scale as p_T^{-4}: (a) $\gamma\gamma \to q\bar{q}$, (b) $\gamma\gamma \to q\bar{q}g$, (c) $\gamma\gamma \to q\bar{q}q\bar{q}$ and $q\bar{q}gg$, (d) $\rho\rho \to q\bar{q}q\bar{q}$ multiplied by 10^3. Curves (e) and (f) give the results of calculating (b) and (c) respectively with the full QCD perturbative structure function $G_{q/\gamma}$.

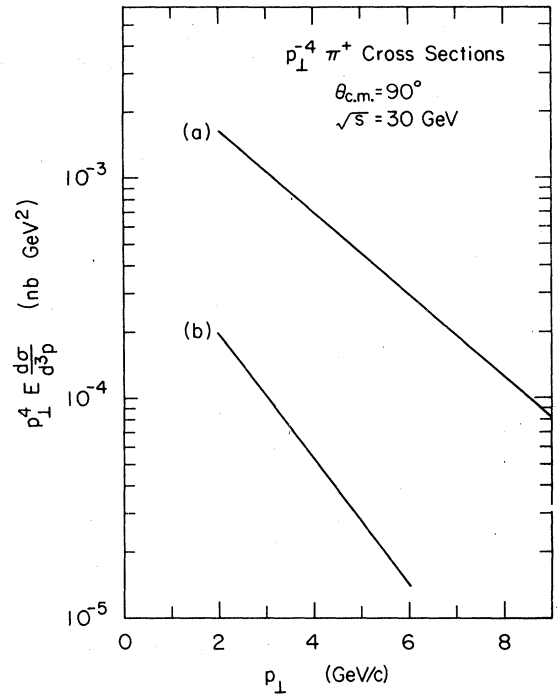

FIG. 7. Single-π^+ inclusive cross sections which scale as p_T^{-4}: (a) $\gamma\gamma \to q\bar{q}$ (b) $\gamma\gamma \to q\bar{q}q\bar{q}$.

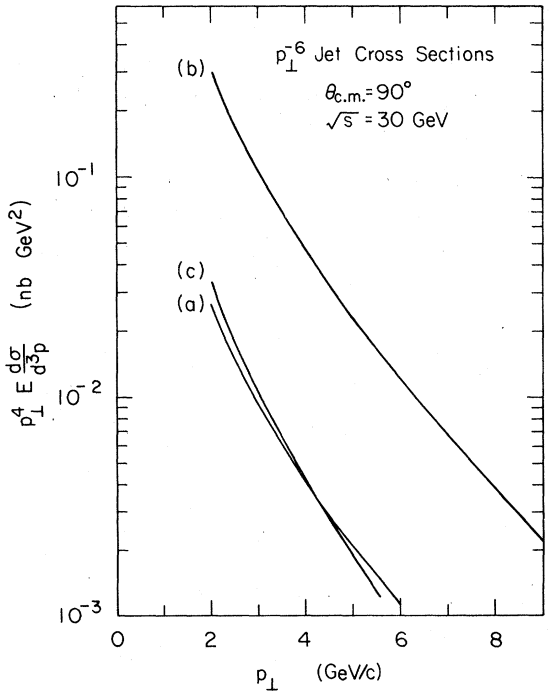

FIG. 8. p_T^{-6} jet cross sections (a) $\gamma\rho \to q\bar{q}$, (b) $\gamma\gamma \to Mq\bar{q}$, (c) $\gamma\rho \to Mq\bar{q}$.

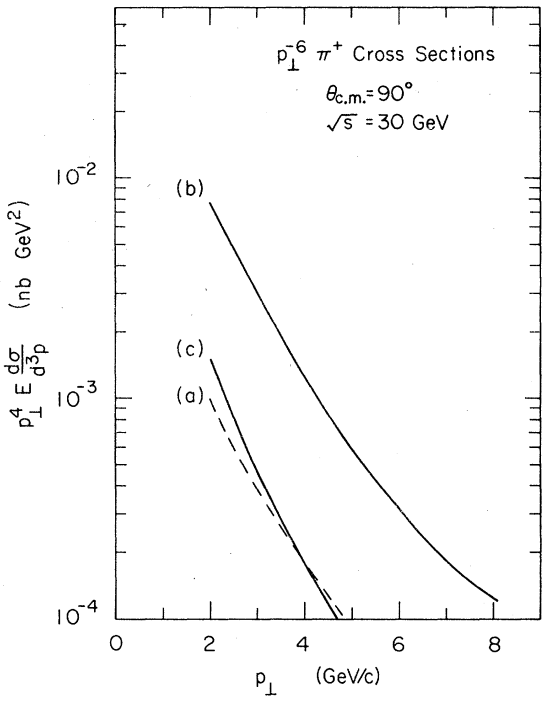

FIG. 9. p_T^{-6} π^+ cross sections (a) $10\times(\gamma p\to q\bar{q})$, (b) $\gamma\gamma\to\pi^+q\bar{q}$, (c) $\gamma p\to\pi^+q\bar{q}$.

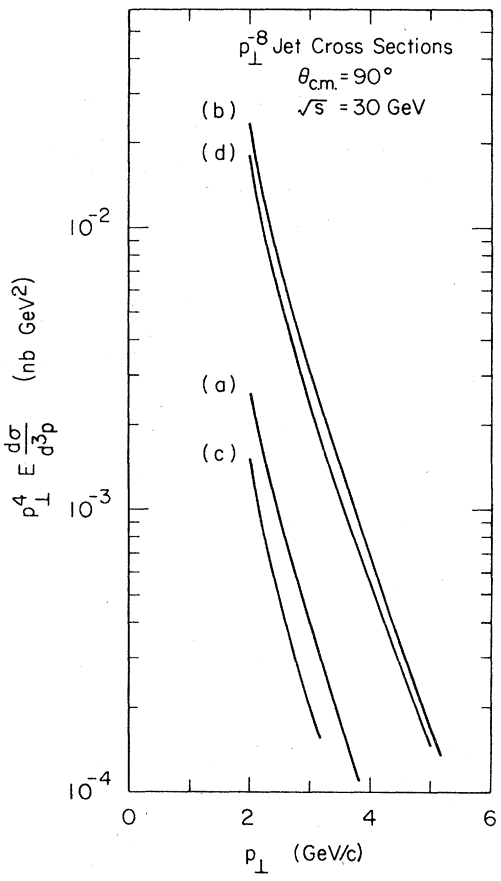

FIG. 10. p_T^{-8} jet cross sections (a) $pp\to q\bar{q}$, (b) $\gamma\gamma\to q\bar{q}M\bar{M}$, (c) $pp\to Mq\bar{q}$, (d) $\gamma p\to Mq\bar{q}$.

haps the simplest hadron-hadron reaction to consider in QCD. We will generally classify contributions according to their topological jet structure and nominal scaling power of p_T^{-n} at fixed x_R and $\theta_{c.m.}$. For convenience in making predictions for experiments at PETRA and PEP we will generally give predictions at $\sqrt{s}$ =30 GeV, and $\theta_{c.m.}$ =90°. The results for other kinematics can be obtained from the scaling laws given in Secs. II and III. When the cross sections for $ee\to$ jet $+X$ or $ee\to H+X$ are written in terms of p_T and $x_R=2p_{\text{trigger}}/\sqrt{s}$, the additional dependence on $\theta_{c.m}$ is not very dramatic. The choice of $\theta_{c.m.}$ =90° is convenient for detectors which surround the interaction region in a e^+e^- colliding-beam experiment but have poor detection efficiency at small angles to the beam. For clarity we will plot $p_T^4\, Ed\sigma/d^3p$ for each inclusive reaction.

The jet cross sections which nominally scale as p_T^{-4} at fixed $\theta_{c.m.}$ and x_R are shown in Fig. 6. The dominant cross section is predicted to be the two-jet $\gamma\gamma\to q\bar{q}$ channel. As we have noted, the magnitude and scaling properties of this cross section [curve 6(a)] are crucial tests of QCD at short distances, checking the asymptotic approach to scale invariance as well as the color and e_q^4 factors in $R_{\gamma\gamma}$ [see Eq. (3.5)]. It is most advantageous to compare the $e^+e^-\to$ jet + jet + e^+e^- rate with $e^+e^-\to\mu^+\mu^-e^+e^-$ since corrections due to the two-photon tagging efficiency and the equivalent-photon approximation tend to cancel.

Curves 6(b) and 6(c) give the jet cross sections from the three-jet and four-jet QCD subprocesses, respectively, as computed using the naive form of $G_{q/e}$ given in Eq. (3.10) with an initial normalization choice $\alpha_c(p_T^2)\,F_Q=1.2$. The full QCD form allowing for gluon bremsstrahlung to all orders along the incident quark directions gives the cross sections shown in 6(e) and 6(f) for the contributions of the three-jet ($\gamma q\to gq$, etc.) and four-jet ($qq\to qq$, etc.) subprocesses. We see that the full QCD form and the simplified Born calculations would be in fairly good agreement if we choose

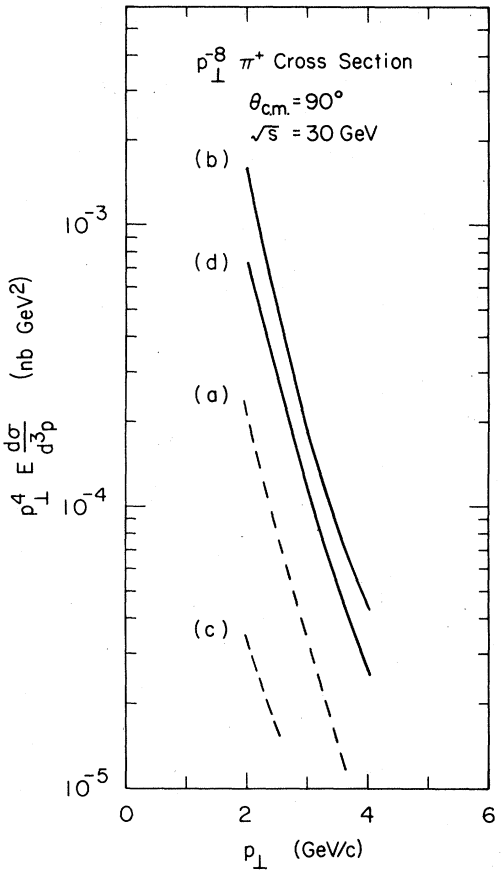

FIG. 11. p_T^{-8} π^+ cross sections (a) $10\times(\rho\rho\to q\bar{q})$, (b) $\gamma\gamma\to\pi Mq\bar{q}$, (c) $10\times(\rho\rho\to\pi q\bar{q})$, (d) $\gamma\rho\to\pi q\bar{q}$.

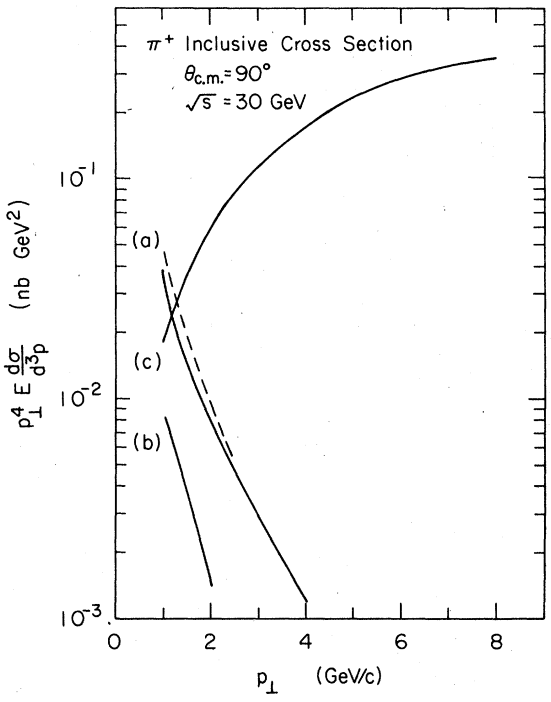

FIG. 12. Combined inclusive π^+ cross section, showing the most important terms, which are the p_T^{-6} (a) $\gamma\gamma\to\pi q\bar{q}$ and (b) $\gamma\rho\to\pi qq$ contributions. Their envelope is given by the dotted line. Also shown is (c) the $e^+e^-\to\gamma\to\pi^+X$ inclusive cross section for comparison. Again, $\sqrt{s}=30$ GeV, $\theta_{c.m.}=90°$.

$\alpha_c(p_T^2)\,F_Q = 0.8$.

We also show the four-jet contribution to the jet cross section from the ρ-dominance contribution, $\rho\rho\to q\bar{q}q\bar{q}$ with $qq\to qq$ scattering, in Fig. 6(d). This contribution is negligible compared to the perturbative QCD contributions.

The various contributions to $p_T^4 E d\sigma/d^3p$ ($ee\to\pi^+X$) from p_T^{-4} reactions as computed in Sec. III are shown in Fig. 7. The p_T^{-6} scaling CIM contributions are shown in Fig. 8 for jets and Fig. 9 for single-π^+ triggers. The p_T^{-8} scaling cross sections for jets and single π^+ triggers are graphed in Figs. 10 and 11, respectively.

The single-π^+ trigger cross sections are more than an order of magnitude smaller than the jet trigger rates. For p_T smaller than ~ 8 GeV, and $\sqrt{s}$ = 30 GeV, p_T^{-6} contributions such as $\gamma q\to\pi q$ where the pion is produced directly in the subprocess is predicted to dominate over the p_T^{-4} processes. This is the result of the "trigger bias" effect[21]: The scale-invariant reactions produce fast quarks in the final state which fragment into slower moving pions. Since the $G_{\pi/q}$ spectrum falls rapidly, the quark p_T is significantly larger than the trigger p_T and the resulting p_T^{-4} production cross section turns out to be suppressed by about two orders of magnitude. The reaction $\gamma q\to\pi q$ produces the pion directly without the need for cascade and this has no trigger bias suppression factor. We present our predictions for the inclusive π^+ spectrum in Fig. 12, together with the single-γ π^+ inclusive cross section as a comparison. Note that, in the absence of tagging, the $\gamma\gamma$ reaction is a dangerous background to the single-γ inclusive-π spectrum at 90° for $x_T < 0.2$, $\sqrt{s}$ = 30 GeV.

We can now plot differential jet cross sections as they might be seen in various sorts of detection schemes.

1. No tagging, central detector. Detectors of this type will be unable to differentiate between

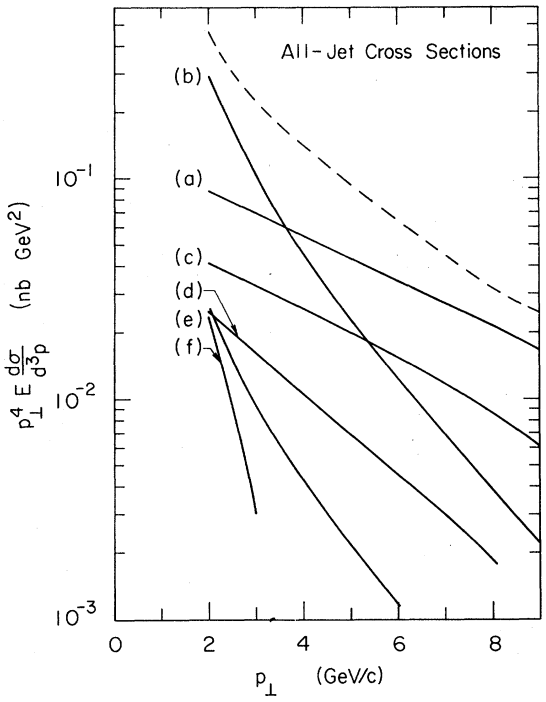

FIG. 13. Jet inclusive cross sections as they would be observed in a central detector without tagging additional forward-backward hadronic jets. The dotted line is the envelope of the most important terms (a) $\gamma\gamma \to q\bar{q}$, (b) $\gamma\gamma \to M q\bar{q}$, (c) $\gamma\gamma \to q\bar{q}g$, (d) $\gamma\gamma \to q\bar{q}q\bar{q}$, (e) $\gamma p \to q\bar{q}$, (f) $\gamma\gamma \to M\bar{M}q\bar{q}$.

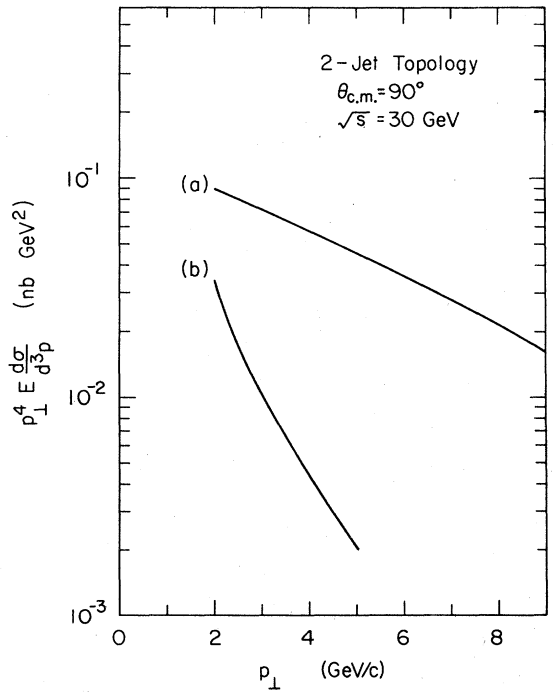

FIG. 14. Dominant jet inclusive cross sections with a two-jet topology (a) $\gamma\gamma \to q\bar{q}$, (b) $\gamma p \to q\bar{q}$.

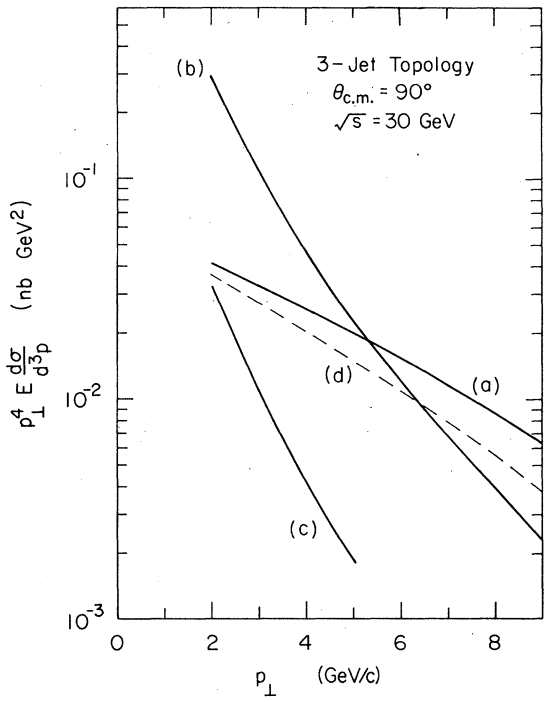

FIG. 15. Jet cross sections, three-jet topology (a) $\gamma\gamma \to q\bar{q}g$, (b) $\gamma\gamma \to Mq\bar{q}$, (b) $\gamma p \to Mq\bar{q}$, (d) $\gamma\gamma \to q\bar{q}g$, computed with the full perturbative structure functions $G_{q/\gamma}$.

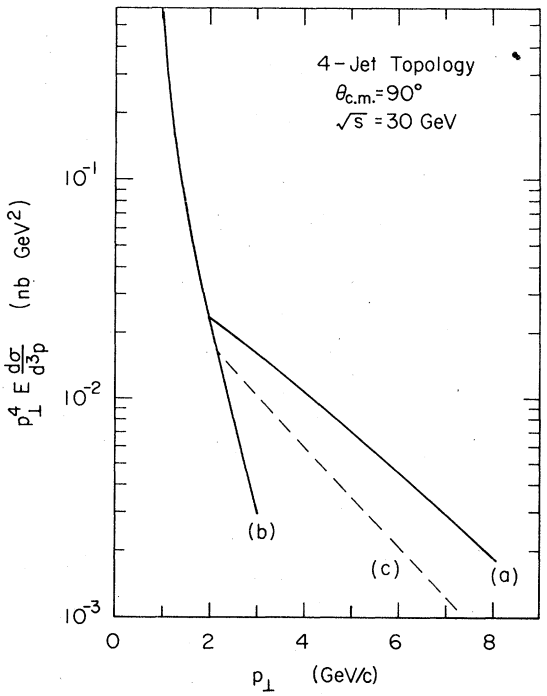

FIG. 16. Jet cross sections, four-jet topology (a) $\gamma\gamma \to q\bar{q}q\bar{q}$ (Born approximation) (b) $\gamma\gamma \to q\bar{q}M\bar{M}$, (c) $\gamma\gamma \to q\bar{q}q\bar{q}$, computed with the full perturbative structure function $G_{q/\gamma}$.

large-p_T events without hadronic jets along the beam direction and those events with accompanying jets. Figure 13 shows the expected jet cross sections which will be observed by such a detector, taken from the largest subprocesses of the preceding figures, and the resulting envelope of the sum of all contributions. The jet spectrum will show a p_T^{-6} falloff up to about $p_T = 4.5$ GeV/c at which point it will "bend" into a p_T^{-4} $(1-x_T)$ shape. Essentially no contributions from gluon jets or gluon exchange are visible.

2. Use of forward photon and hadron tagging with a central detector. Experiments of this type have the great advantage that one can, in principle, trigger on events with a particular number of small-p_T jets in addition to large-p_T jets. This considerably simplifies the problem of differentiating the various types of hard-scattering reactions which occur. The useful quantities to present here are inclusive jet cross sections with two, three, or four hadronic jets, shown in Figs. 14, 15, and 16, respectively. (No corrections for tagging efficiency for either electrons or hadrons have been included.)

The ability to differentiate subprocesses is dramatically improved by the inclusion of a forward detector. The two-jet reaction is dominated by the process $\gamma\gamma \to q\bar{q}$ for $p_T > 2$ GeV/c. The four-jet cross section is dominated by the p_T^{-4} process $\gamma\gamma \to q\bar{q}q\bar{q}$ for $p_T > 2$ GeV. The three-jet cross section is dominated by the p_T^{-6} reaction $\gamma\gamma \to Mq\bar{q}$ out to $p_T = 2$ GeV, but remains important for the entire range of momenta accessible to experiments at $\sqrt{s} = 30$ GeV.

The jet cross section integrated over transverse momenta is quite large, even for the single particular subprocess $\gamma\gamma \to q\bar{q}$ (which we expect will dominate at large p_T). The integrated cross section for jets with trigger momentum larger than $p_T^{\min}$ is[2]

$$\sigma\left(p_T > p_T^{\min}\right) = \int_{p_T > p_T^{\min}} d^2p_T \int dy \, \frac{E\,d\sigma}{d^3p} \quad (e^+e^- \to e^+e^- + q\bar{q} \text{ or } \bar{q}q) \tag{4.1}$$

$$\approx \frac{32\pi}{3}\,\alpha^2 \left(\frac{\alpha}{2\pi} \ln \eta\right)^2 R_{\gamma\gamma} \frac{\left(\ln \frac{s}{(p_T^{\min})^2} - \frac{19}{6}\right)}{(p_T^{\min})^2} \tag{4.2}$$

which is the result of an analytic integration assuming $xG_{\gamma/e}(x) \sim (\alpha/\pi)\ln\eta]$, or about 0.5 nb GeV^2/$(p_T^{\min})^2$ at $\sqrt{s} = 30$ GeV. Jets with $p_T > 4$ GeV contribute 0.3 more units of R to the e^+e^- total cross section at $\sqrt{s} = 30$ GeV from this process alone.

We emphasize that $\gamma\gamma \to q\bar{q}$ events will be observed in central detectors even in the absence of electron tagging. These hadronic events will appear as two "short" jets (visible energy much less than $E_{\text{c.m.}}$), which are coplanar, roughly balanced in transverse momentum, and in general are not back-to-back in angle. As we have noted, single hadrons arising from $\gamma\gamma$ collisions at high p_T will be a serious background to single-hadron e^+e^- annihilation physics for x_R below about 0.2 but are negligible above that value. A good way to reduce contamination of one-γ physics from two-γ processes will be to require the observation of at least one hadron in the former reactions with $x_R > 0.2$ or so, or require a calorimetric trigger with $E_{\text{vis}} \approx E_{\text{c.m.}}$.

Of course, the best way to study $\gamma\gamma$ events is with an electron-hadron forward tagging detector, used not so much to measure the energy of the electrons or hadrons as to simply indicate that a $\gamma\gamma$ interaction has taken place. A single tagged electron will suffice for such a trigger, although double tagging may be necessary to remove machine-related backgrounds. If one is then left with a clean enough sample of events, one can then sift them to analyze separate multijet contributions to the jet and single-particle cross sections.

V. CONCLUSIONS AND DISCUSSIONS

We conclude by summarizing our predictions:

1. The cross section for producing jets at large p_T from $\gamma\gamma$ collisions is large: $\sigma(p_T > 3\ \text{GeV}) \simeq 0.05$ nb at $\sqrt{s} = 30$ GeV.

2. The dominant contribution to the $e^+e^- \to e^+e^-$ jet cross section at $p_T > 4$ GeV/c is the pointlike reaction $\gamma\gamma \to q\bar{q}$, whose magnitude is absolutely normalized to be proportional to the $\gamma\gamma \to \mu^+\mu^-$ cross section. The constant of proportionality is $R_{\gamma\gamma} = 3\sum e_i^4$. Observation of this reaction and its characteristic scale-invariant behavior will represent the first direct verification of the $1/\not{p}$ shape of the quark propagator. It will also be interesting to study the logarithmic approach to scaling predicted by quantum chromodynamics and the effects of heavy-quark-antiquark thresholds.

3. The single-π cross section has a behavior $Ed\sigma/d^3p\ (e^+e^- \to e^+e^-\pi X) \propto (1 - x_R)^2 p_T^{-6}$ and represents a sizable background to single-photon-induced hadroproduction for $x_R < 0.2$. The magnitude of the leading contribution is fixed by the constituent-interchange model and its measurement is a check of that model.

4. A rich jet structure—two, three, and four hadronic jets—will be exposed to detectors and tagging counters aligned at small angles to the beam. In particular, the four-jet cross section holds the possibility of seeing quark-quark scattering by vector-gluon exchange. The even larger three-jet cross section allows the study of gluon jets and the QCD Compton process $\gamma q \to gq$.

5. Processes in which the photons vector-dominate into low-mass states before scattering are essentially a negligible component of the large-p_T cross section, although they give the dominant contribution for small p_T.

Since these reactions are not small and since they represent such a rich laboratory for the investigation of quark and hadron dynamics, it is important that a considerable effort be made to study them. The simpler form of 4π solid-angle detectors will be able to elucidate the general features of these reactions. Detailed dynamical questions, such as the number of jets produced in a given interaction, require information which is most easily obtained from a forward tagging system used in conjunction with a central detector.

We must emphasize that this work represents only a first survey of the field of $\gamma\gamma$-induced jet reactions. Many interesting problems remain to be studied. On the side of phenomenology, for instance, tagging the electrons provides information on the scattering of *polarized* photons into jets—for which the simplest process $\gamma\gamma \to q\bar{q}$ will give unique predictions. One may study quantum-number correlations between fast hadrons in one large-p_T jet and fast hadrons in the other jet, which will differ in $\gamma\gamma \to q\bar{q}$ from the correlations seen in $\gamma^* \to q\bar{q}$ because of the different charge structure.

The occurrence of $\gamma\gamma$ reactions at an experimentally observable level implies that the entire range of hadronic physics which can be studied, for example, at the CERN ISR can also be studied in parallel in $e^\pm e^-$ machines. Although low-p_T $\gamma\gamma$ reactions should strongly resemble meson-meson collisions, the elementary-field nature of the photon implies dramatic differences at large p_T. This region can be a crucial testing ground for QCD since not only are a number of new subprocesses accessible ($\gamma\gamma \to q\bar{q}$, $\gamma q \to gq$, $\gamma q \to Mq$, etc.) and predicted with essentially with no free parameters, but most important, one can make predictions for a major component of the photon structure function directly from QCD. We also note that there are open questions in hadron-hadron collisions, e.g., whether nonperturbative effects (instantons, wee-parton interactions) are important for large-p_T reactions.[6] Such effects are presumably absent for the perturbative, pointlike interactions of the photon. We also note that the interplay between vector-meson dominance and pointlike contributions to the hadronic interactions of the photon is not completely understood in QCD, and $\gamma\gamma$ processes may illuminate these questions.

As a final point, we wish to remark that even though we have been mainly concerned with e^+e^- colliding beams in the $\sqrt{s} = 30$ region, the $\gamma\gamma$ processes become even more important as the center-of-mass energy is increased. There has already been some talk of construction of an e^+e^- storage ring with $\sqrt{s} \sim 200$ GeV. At this energy, one unit of R of cross section is about 2.25×10^{-3} nb, whereas the integrated cross section for the process $e^+e^- \to e^+e^-q\bar{q}$ with $p_T > 10$ GeV is ~ 0.02 nb, or about 9 units of R. These estimates speak for themselves: Very energetic e^+e^- colliding-beam machines are more nearly laboratories for $\gamma\gamma$ scattering than they are for e^+e^- annihilation.

ACKNOWLEDGMENTS

We would like to thank J. D. Bjorken, R. Blankenbecler, and the members of the PEP-9 collaboration at Davis and Santa Barbara for discussions. J.G. and J.W. have been recipients of A.P. Sloan Foundation Fellowships. This work was supported in part by the Department of Energy under Contract No. EY-76-C-03-0515. The final version of this paper was completed after the tragic death of our colleague, J. H. Weis.

APPENDIX A: DERIVATION OF CONVOLUTION FORMULAS

We consider the process shown in Fig. 17 where the fragments a and b of particles A and B undergo a hard scattering to produce the particles c and d. The particle c subsequently fragments to form C. In the applications discussed in this paper A and B are the incident e^+ and e^-, C is an observed meson, and a and b can be either photons, ρ mesons, or quarks. The relevant fragmentation functions and cross sections $d\sigma/dt$ are given in the text.

We first derive[7] the inclusive cross section $Ed\sigma/d^3p$ for the process $A+B\to C+X$ and then specialize it to the case where the fragmentation of c is absent.

Cross sections are conveniently derived using the notation of Ref. 3. We assume throughout that all particles are ultrarelativistic ($E_i \simeq |\vec{p}_i|$). We define the momentum fractions in the c.m. frame of A and B:

$$x_R \equiv 1-\epsilon = \frac{2|\vec{p}_C|}{\sqrt{s}}, \quad x_F = \frac{2p_C{}^3}{\sqrt{s}} \tag{A1}$$

and

$$x_t = \frac{-t}{s} \equiv \frac{(p_A - p_C)^2}{(p_A+p_B)^2} = \tfrac{1}{2}(x_R - x_F),$$

$$x_u = -\frac{u}{s} \equiv \frac{(p_B - p_C)^2}{(p_A+p_B)^2} = \tfrac{1}{2}(x_R + x_F). \tag{A2}$$

Similarly for the subprocess we define

$$\hat{x}_t \equiv -\frac{\hat{t}}{\hat{s}} = \frac{(p_a - p_c)^2}{(p_a+p_b)^2},$$

$$x_u \equiv -\frac{\hat{u}}{\hat{s}} = \frac{(p_b - p_c)^2}{(p_a+p_b)^2}, \tag{A3}$$

$$\hat{x} \equiv \frac{2|\vec{p}_c|}{\sqrt{s}}.$$

Following Ref. 3, the probability of the whole process is given by the product of the probabilities of the subprocesses. Writing the probability of finding a constituent a in A with (light-cone/infinite-momentum-frame) momentum fraction between x_a and x_a+dx_a as $G_{a/A}(x_a)dx_a$, we have

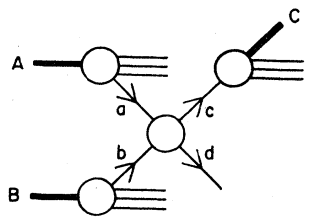

FIG. 17. The standard hard-scattering parton-model diagram for $AB\to CX$.

$$d\sigma = \int\int\int dx_a\, G_{a/A}(x_a)\, dx_b\, G_{b/B}(x_b) \times \left(\frac{d\sigma}{d\hat{x}_t\, d\hat{x}_u}\, d\hat{x}_t\, d\hat{x}_u\right) G_{C/c}(x_C) dx_C, \tag{A4}$$

where

$$x_C \equiv \frac{|\vec{p}_C|}{|\vec{p}_c|}. \tag{A5}$$

Since $m_d{}^2 \ll \hat{s}$, $\hat{x}_u+\hat{x}_t \simeq 1$ and

$$\frac{d\sigma}{d\hat{x}_t\, d\hat{x}_u} = \hat{s}\frac{d\sigma}{d\hat{t}}\delta(1-\hat{x}_t-\hat{x}_u). \tag{A6}$$

Furthermore, it is easy to show[3] that

$$\hat{x}_t = \frac{1}{x_C x_b}x_t, \quad \hat{x}_u = \frac{1}{x_C x_a}x_u, \tag{A7}$$

and

$$d\hat{x}_t\, d\hat{x}_u = \frac{1}{x_C{}^2 x_a x_b}\, dx_t\, dx_u = \frac{1}{x_C{}^2 x_a x_b}\,\frac{1}{\pi s}\,\frac{d^3p_c}{E_c}. \tag{A8}$$

Inserting these in (A4) gives[3]

$$E_C\frac{d\sigma}{d^3p_C} = \int_0^1\int_0^1 dx_a\, dx_b\, G_{a/A}(x_a)G_{b/B}(x_b)\,\frac{\hat{s}}{\pi}\frac{d\sigma}{d\hat{t}}\,\frac{G_{C/c}(x_C)}{x_C{}^2}\, dx_C\,\theta(1-x_C)\Big|_{x_C = x_t/x_b + x_u/x_a}. \tag{A9}$$

We now assume explicit simple forms for the fragmentation functions:

$$G_{i/I}(x_i) = (1+g_i)\Lambda_{i/I}\frac{(1-x_i)^{g_i}}{x_i} \tag{A10}$$

and

$$\frac{d\sigma}{d\hat{t}} = \pi D\,\hat{s}^{-N}(\hat{x}_t)^{-T}(\hat{x}_u)^{-U}\ . \tag{A11}$$

Inserting (A10) and (A11) in (A8) we obtain

$$E_C\frac{d\sigma}{d^3p_C} = \frac{x_t^{-T}x_u^{-U}}{s^N}D\Lambda_{a/A}\Lambda_{b/B}\Lambda_{C/c}(1+g_a)(1+g_b)(1+g_c)$$
$$\times\int_0^1\int_0^1 dx_a\,dx_b\,(1-x_a)^{g_a}(1-x_b)^{g_b}x_a^{U-N-1}x_b^{T-N-1}x_C^{T+U-2}(1-x_C)^{g_c}\theta(1-x_C)\Big|_{x_C=x_t/x_a+x_u/x_b}\ . \tag{A12}$$

Equation (A12) can be put into a more convenient form by changing variables so that the triangular integration region becomes the unit square:

$$x_a = \left(1+\frac{\epsilon z y}{x_u}\right)^{-1},\quad x_b = \left(1+\frac{\epsilon z(1-y)}{x_t}\right)^{-1}\ . \tag{A13}$$

We thus obtain

$$E_C\frac{d\sigma}{d^3p_C} = \frac{\epsilon^{g_a+g_b+g_C+2}}{(p_T^2)^N}D\Lambda_{a/A}\Lambda_{b/B}\Lambda_{C/c}(1+g_a)(1+g_b)(1+g_c)2^{g_a+g_b+T+U+2-2N}$$
$$\times\int_0^1\int_0^1 dz\,dy\,z^{g_a+g_b+1}(1-z)^{g_c}y^{g_a}(1-y)^{g_b}[1-\epsilon(1-z)]^{T+U-2}[1+x_F-\epsilon(1-2zy)]^{N-U-g_a-1}$$
$$\times\{1-x_F-\epsilon[1-2z(1-y)]\}^{N-T-g_b-1}\ . \tag{A14}$$

This is the basic formula we use in our numerical calculations. We note that for small ϵ the final three factors in the integral are approximately unity and[7]

$$E_C\frac{d\sigma}{d^3p_C} \underset{\epsilon\to 0}{\sim} \frac{\epsilon^{g_a+g_b+g_C+2}}{(p_T^2)^N}D\Lambda_{a/A}\Lambda_{b/B}\Lambda_{C/c}\,2^{g_a+g_b+T+U+2-2N}\,\frac{\Gamma(g_a+2)\Gamma(g_b+2)\Gamma(g_c+2)}{\Gamma(3+g_a+g_b+g_c)}\ . \tag{A15}$$

If g_a and g_b are large while g_c is small, $y\approx\frac{1}{2}$ and $z\approx 1$ will dominate in (A14) and the final factors are approximately

$$(1+x_F)^{N-U-g_a-1}(1-x_F)^{N-T-g_b-1}\ ,$$

but this is not the situation encountered here.

When the fragmentation of c is not present, the analog of (A12) is

$$E_c\frac{d\sigma}{d^3p_c} = \frac{x_t^{-T}x_u^{-U}}{s^N}D\Lambda_{a/A}\Lambda_{b/B}(1+g_a)(1+g_b)\int_0^1\int_0^1 dx_a\,dx_b\,(1-x_a)^{g_a}(1-x_b)^{g_b}x^{U-N-1}x_b^{T-N-1}\delta\left(1-\frac{x_t}{x_b}-\frac{x_u}{x_a}\right)\ , \tag{A16}$$

which upon using (A13), gives

$$E_c\frac{d\sigma}{d^3p_c} = \frac{\epsilon^{g_a+g_b+1}}{(p_T^2)^N}D\Lambda_{a/A}\Lambda_{b/B}(1+g_a)(1+g_b)2^{g_a+g_b+T+U+2-2N}$$
$$\times\int_0^1 dy\,y^{g_a}(1-y)^{g_b}[1+x_F-\epsilon(1-2y)]^{N-U-g_a-1}[1-x_F+\epsilon(1-2y)]^{N-T-g_b-1}\ . \tag{A17}$$

For $\epsilon \to 0$, we have

$$\frac{E\,d\sigma}{d^3p} \sim \frac{\epsilon^{g_a+g_b+1}}{(p_T^2)^N} D\Lambda_{a/A}\Lambda_{b/B} \frac{\Gamma(2+g_a)\Gamma(2+g_b)}{\Gamma(2+g_a+g_b)} 2^{g_a+g_b+T+U+2-2N}. \tag{A18}$$

This is actually exact for the dominant term in CIM process $\gamma q \to qM$ ($a=\gamma$, $b=q$, $c=M$, $d=q$) since $N-U-g_a-1=N-T-g_b-1=0$. For small x_F and ϵ the integrand of Eq. (A17) can be expanded. For example, this leads to corrections to (A18) of

$$[1+2x_F+x_F^2+\tfrac{2}{3}\epsilon^2+O(\epsilon^3, \epsilon^2 x_F, x_F^3, \text{ etc})]$$

for the QED process ($a=b=\gamma$, $c=d=q$).

APPENDIX B: QCD EFFECTS IN $\gamma\gamma$ COLLISIONS

Perturbative corrections modify Born approximation calculations for $\gamma\gamma$ collisions such as the $qq \to qq$ and $\gamma q \to gq$ subprocesses in two mutually compensating ways. First, the running coupling constant asymptotically varies with the p_T of the subprocess as[22]

$$\alpha_c(p_T^2) \cong \frac{1}{b\ln(p_T^2/\Lambda^2)}, \tag{B1}$$

where $4\pi b = 11 - \frac{2}{3}n_f$ for color SU(3) and n_f flavors. Second, the distributions of quarks in photons (and electrons) are modified, as was first discussed by Witten.[4,5] For our purposes it will be sufficient to retain only the "nonsinglet" contributions to the photon structure functions, analogous to the valence quark contributions of the proton. The approximation is justified for our large-p_T applications because the singlet or quark sea contributions (from gluon bremsstrahlung and pair production) vanish two powers faster in $(1-x)$. This is an especially useful approximation because it obviates the need to perform operator mixing or to redo the complicated quark charge counting of Sec. II.

Within the valence approximation we can use the convolution form (see also Ref. 15)

$$G_{q/\gamma}(x,Q^2) = \frac{3\alpha}{2\pi} e_q^2 \int_{\mu^2}^{Q^2} \frac{dk^2}{k^2} \int_x^1 \frac{dz}{z} [z^2+(1-z)^2] \times G_{q/q}\left(\frac{x}{z}, Q^2, k^2\right), \tag{B2}$$

where $G_{q/q}$ is the standard nonsinglet distribution for quarks in a target quark of mass k^2 being probed at four-momentum squared Q^2. The factor of 3 includes the sum over color. We shall assume that the contribution from $k^2 < \mu^2$ is accounted for by the vector-meson-dominance contributions. Taking moments, we have

$$G_{q/\gamma}(j,Q^2) = \frac{3\alpha}{2\pi} e_q^2 \int_{\mu^2}^{Q^2} \frac{dk^2}{k^2} f(j) G_{q/q}(j,Q^2,k^2), \tag{B3}$$

where

$$G(j) \equiv \int_0^1 dx\, x^{j-1} G(x), \tag{B4}$$

$$f(j) = \int_0^1 dz\, z^{j-1}[z^2+(1-z)^2] = \frac{1}{j} - \frac{2}{j+1} + \frac{2}{j+2}, \tag{B5}$$

and

$$G_{q/q}(j,Q^2,k^2) = \left[\frac{\alpha(k^2)}{\alpha(Q^2)}\right]^{d_j/2\pi b} \tag{B6}$$

The d_j are the standard valence anomalous dimensions, as defined in Ref. 23. Evaluating the k^2 integral in (B3) yields

$$G_{q/\gamma}(j,Q^2) = \frac{3}{2\pi} e_q^2 \frac{\alpha}{\alpha_c(Q^2)} \left[\frac{2\pi f(j)}{2\pi b - d_j}\right]. \tag{B7}$$

This exhibits the remarkable scaling features of the photon structure function discussed in Sec. III.

It is easy to invert the moment Eq. (B7) via the method of Yndurian.[24] A graph of $xG_{q/\gamma}(x)$ calculated in valence approximation in QCD and in the parton model is given in Fig. 1(b). Good agreement is obtained with the exact (valence plus

singlet) results of Llewellyn Smith[5] over nearly the entire range of x.

The x near 1 behavior of $G_{q/\gamma}(x)$ can be obtained more directly from a direct integration of (B2), using the $x \to 1$ form for the quark structure function[15]

$$G_{q/q}(x, Q^2, k^2) = \exp[(3-4\gamma_E)\xi C_2](1-x)^{4C_2\xi-1}/\Gamma(4C_2\xi) , \tag{B8}$$

where $\gamma_E = 0.577\ldots$ is Euler's constant, $C_2 = (N^2-1)/2N = \frac{4}{3}$, and

$$\xi = \frac{1}{4\pi b} \ln \frac{\alpha(k^2)}{\alpha(Q^2)} . \tag{B9}$$

We then obtain[15]

$$G_{q/\gamma}(x, Q^2) \underset{x\to 1}{=} \frac{3}{2\pi} e_Q^{\,2} \frac{\alpha}{\alpha_c(Q^2)} \times \frac{4\pi}{4\pi b - (3-4\gamma_E)C_2 + 4C_2 \ln[1/(1-x)]} . \tag{B10}$$

This result is numerically accurate only for $x \gtrsim 0.97$ but is off by no more than a factor of 2 for $x > 0.1$ (see Fig. 1).

Finally, as we are interested in electron-electron scattering, we most convolute $G_{q/\gamma}(x)$ and $G_{\gamma/e}(x)$. That is most easily done, once again, by taking moments and using Yndurian's method. We find

$$G_{q/\gamma/e}(x, Q^2) = 3\left(\frac{\alpha}{2\pi}\right)^2 e_q^{\,2} \frac{\ln\eta}{\alpha_c(Q^2)} \frac{1-x}{x} \tilde{f}(x) \tag{B11}$$

where $\hat{f}(x)$ is shown in Fig. 1(d). The $x \to 1$ behavior of $\tilde{f}(x)$ is given in Sec. III.

---

*Present address: Department of Physics, University of California, Santa Barbara, Calif. 93106.

[1]S. J. Brodsky, T. Kinoshita, and T. Terazawa, Phys. Rev. D 4, 1532 (1971). For reviews see V. M. Budnev *et al.*, Phys. Rep. 15C, 181 (1975); H. Terazawa, Rev. Mod. Phys. 45, 615 (1973); the reports of S. Brodsky, H. Terazawa, and T. Walsh in proceedings of the International Colloquium on Photon-Photon Collisions in Electron-Positron Storage Rings, Collège de France, Paris [J. Phys. (Paris) Suppl. 35, C2-1 (1974)].

[2]A short report of this work is given in S. J. Brodsky, T. DeGrand, J. F. Gunion, and J. Weis, Phys. Rev. Lett. 41, 672 (1978). A calculation of 2γ processes in QCD is also being carried out by C. H. Llewellyn Smith and collaborators (private communication).

[3]The $\gamma\gamma \to q\bar{q}$ process for single-hadron production at large p_T in e^+e^- collisions was first considered in the pioneering paper by J. D. Bjorken, S. Berman, and J. Kogut, Phys. Rev. D 4, 3388 (1971). A discussion of this process for virtual γ reactions has been given by T. F. Walsh and P. Zerwas, Phys. Lett. 44B, 195 (1973).

[4]E. Witten, Nucl. Phys. B120, 189 (1977).

[5]The results of Witten have been rederived by summing ladder graphs by W. Frazer and J. Gunion [Phys. Rev. D (to be published)] and by C. H. Llewellyn Smith, Oxford Report No. 67/78 (unpublished), and Phys. Lett. 79B, 83 (1978). See also Ref. 15.

[6]We wish to thank J. Ellis for conversations on this point.

[7]R. Blankenbecler, S. Brodsky, and J. F. Gunion, Phys. Rev. D 18, 900 (1978), and references therein.

[8]For a comprehensive review of the vector-meson-dominance model see T. H. Bauer, R. D. Spital, and D. R. Yennie, Rev. Mod. Phys. 50, 261 (1978). For an early discussion of the phenomenological necessity for a perturbative, pointlike component for photon-induced reactions see S. J. Brodsky, F. E. Close, and J. F. Gunion, Phys. Rev. D 6, 177 (1972). The relationship between pointlike parton-model contributions and the infinite vector-meson spectrum is discussed by S. J. Brodsky and J. Pumplin, Phys. Rev. 182, 1794 (1969); V. N. Gribov, report from the Fourth Winter Seminar of the Theory of the Nucleus and the Physics, Acad. Sci. (USSR), 1969 (unpublished); E. Etim, M. Greco, and Y. Srivastava, Lett. Nuovo Cimento 16, 65 (1976); J. D. Bjorken, in *Proceedings of the International Symposium on Electron and Photon Interactions at High Energies*, edited by N. B. Mistry (Laboratory of Nuclear Studies, Cornell Univ., Ithaca, N.Y., 1972); S. Brodsky, G. Grammer, G. P. Lepage, and J. D. Sullivan (unpublished).

[9]D. Jones and J. F. Gunion, Phys. Rev. D 19, 867 (1979); J. F. Gunion, University of California Davis Report No. 78/0353, 1978 (unpublished). See also S. J. Brodsky, talk presented at the Conference on Jets in High Energy Collisions, Copenhagen, 1978 (unpublished).

[10]C. Weizsäcker and E. J. Williams, Z. Phys. 88, 612 (1934); R. B. Curtis, Phys. Rev. 104, 211 (1950); R. H. Dalitz and D. R. Yennie, *ibid.* 105, 1598 (1957).

[11]G. Grammer and T. Kinoshita, Nucl. Phys. B80, 461 (1974); R. Bhattacharya, J. Smith, and G. Grammer, Phys. Rev. D 15, 3267 (1977); J. Smith, J. Vermaseren, and G. Grammer, *ibid.* 15, 3280 (1977). Our results are in good agreement with these $e^+e^- \to e^+e^-l\bar{l}$ calculations. We wish to thank J. Vermaseren for making this comparison.

[12]W. Caswell, R. Horgan, and S. J. Brodsky, Phys. Rev. D 18, 2415 (1978).

[13]V. N. Gribov and L. N. Lipatov, Yad. Fiz. 15, 781 (1971) [Sov. J. Nucl. Phys. 15, 438 (1972)], and references therein. For a similar approach to QED structure functions see M. Chen and P. Zerwas, Phys. Rev. D 12, 187 (1975). See also G. Altarelli and G. Parisi, Nucl. Phys. B126, 298 (1977).

[14]It would be interesting to obtain the QCD pertubative corrections to $R_{\gamma\gamma}$ [see Eq. (3.5)] as a function of all the subprocess invariants, $\hat{s}$, t, q_1^2, q_2^2. Related corrections also occur in calculations of the Bjorken-Paschos subprocess $\gamma q \to \gamma q$ for inelastic Compton scattering.

[15]Yu. L. Dokshitser, D. I. Dyankanov, and S. I. Troyan, Stanford Linear Accelerator Center translation SLAC-TRANS-183, translated for Proceedings of the 13th

Leningrad Winter School on Elementary Particle Physics, 1978 (unpublished).
[16]See also K. J. Anderson *et al.*, Enrico Fermi Institute Report No. EFI-78-38 (unpublished) for data on the pion structure function obtained from $\pi^- C \to \mu^+ \mu^- X$. Their results are consistent with the $(1-x)$ power used here.
[17]R. Rückl. S. J. Brodsky, and J. F. Gunion, Phys. Rev. D 18, 2469 (1978).
[18]B. L. Combridge, J. Kripfganz, and J. Ranft, Phys. Lett. 70B, 234 (1977); R. Cutler and D. Sivers, Phys. Rev. D 17, 196 (1978); 16, 679 (1977).
[19]An estimate of the VDM contribution using an extrapolation from $pp \to \text{jet} + X$ data is given in Ref. 2.
[20]R. C Brower, J. Ellis, M. G. Schmidt, and J. H. Weis, Nucl. Phys. B128, 175 (1977) and references therein.
[21]S. D. Ellis, M. Jacob, and P. V. Landshoff, Nucl. Phys. B108, 93 (1976).
[22]H. Georgi and D. Politzer, Phys. Rev. D 9, 419 (1974); D. Gross and F. Wilczek, *ibid.* 9, 980 (1974).
[23]G. Altarelli and G. Parisi, Ref. 13.
[24]F. J. Yndurian, Phys. Lett. 74B, 68 (1978).